공학박사 학위논문

Sensitivity and Uncertainty Analysis of Nuclear Reactor Reactivity Coefficients Due to Nuclear Covariance Data by Monte Carlo Second-Order Perturbation Techniques

몬테칼로 2차 섭동법에 의한 원자로 반응도계수의 핵자료 민감도 및 불확도 분석

2018년 2월

서울대학교 대학원
에너지시스템 공학부
유 승 열

Sensitivity and Uncertainty Analysis of Nuclear Reactor Reactivity Coefficients Due to Nuclear Covariance Data by Monte Carlo Second-Order Perturbation Techniques

몬테칼로 2차 섭동법에 의한 원자로
반응도계수의 핵자료 민감도 및 불확도 분석

지도 교수 심 형 진

이 논문을 공학박사 학위논문으로 제출함
2018년 2월

서울대학교 대학원
에너지시스템 공학부
유 승 열

유승열의 공학박사 학위논문을 인준함
2018년 1월

위 원 장	주 한 규	(인)
부위원장	심 형 진	(인)
위 원	김 봉 기	(인)
위 원	이 현 철	(인)
위 원	김 응 수	(인)

Abstract

The uncertainty quantification of the reactivity coefficients such as the fuel temperature coefficient (FTC) and the moderator density coefficient (MCD) is crucial for the nuclear reactor safety margin evaluation. For the nuclear data sensitivity and uncertainty (S/U) analysis of the reactivity coefficient, this study proposes a new method to efficiently estimate the sensitivities of the reactivity coefficient to cross sections by the Monte Carlo (MC) perturbation techniques. A perturbation formulation for the reactivity coefficient has been derived based on the differential operator sampling method accompanied with the fission source perturbation method (DOS/FSP). In the new formulation, the sensitivity of the reactivity coefficient is expressed by reactivity derivatives with respect to two different variables. The proposed MC second-order perturbation (MC2P) method is implemented into Seoul National University MC code, McCARD.

The proposed MC2P method is verified via sensitivities of the density coefficient and the temperature coefficient in two-group homogeneous infinite medium problems by comparing its results with analytic solutions. The sensitivities estimated by MC2P method agree with the analytic solutions within three standard deviations. The effectiveness of the MC2P method is examined for a ^{235}U density coefficient problem in Godiva by

comparisons with direct subtraction-based approach in which the sensitivities of the reactivity coefficients are estimated by subtracting the first-order k sensitivities in nominal and perturbed systems. From the comparison results, one can see that the new method can predict the cross section sensitivities of the reactivity coefficient more accurately from much smaller number of MC history simulations. Then the proposed method is applied to quantify the uncertainties of the MDC of a LWR pin cell problem and the FTC of a CANDU 6 lattice cell problem due to the nuclear covariance data. The MDC uncertainty of the LWR pin cell problem are estimated as 0.44%. The FTC uncertainty of the CANDU 6 bundle problem is estimated as 1.24%.

Keyword : Sensitivity and Uncertainty, Second-Order Perturbation, Reactivity Coefficient, McCARD

Student Number : 2013-30293

Table of Contents

Chapter 1. Introduction 1

1.1 Background 1

1.2 Objective 4

Chapter 2. Monte Carlo Second-Order Perturbation Method for Sensitvitity Estimation of Reactiavity Coefficient 6

2.1 Derivation 6

2.2 First-Order DOS Method 9

2.3 First-Order FSP Method 13

2.4 Second-Order DOS Method for Two Variables 16

2.5 Second-Order FSP Method for Two Variables 21

2.6 Sensitivity of the Temperature Coefficient 23

Chapter 3. Effectiveness of the MC2P Method 33

3.1 Two-Group Infinite Homogeneous Problem of CANDU 6 Bundle Model 33

3.2 ^{235}U-Density Coefficient in Godiva 53

Chapter 4. Applications for the Reactivity Coefficient S/U Analysis 57

4.1 Nuclear Data S/U Analysis 57

4.2 MDC S/U Analysis for Continuous-Energy PWR Pin Problem 58

4.3 FTC S/U Analysis for Continuous-Energy CANDU 6 Bundle Problem 60

Chapter 5. Conclusion 63

Reference 65

List of Tables

Table 3.1 Two-group macroscopic cross sections for the fuel-coolant mixture of the infinite homogeneous problem 38

Table 3.2 Two-group microscopic cross sections for the moderator of the infinite homogeneous problem 39

Table 3.3 Comparisons of k sensitivities to the moderator density..... 40

Table 3.4 Comparisons of *k* sensitivities to the macroscopic cross sections of fuel-coolant mixture, $\partial k/\partial \Sigma$, for the infinite homogeneous problem..... 41

Table 3.5 Comparisons of the second-order *k* derivatives, $\partial^2 k/\partial \mathrm{N}_{\mathrm{mod}} \partial \Sigma$, for the infinite homogeneous problem 43

Table 3.6 Comparisons of the second-order *k* derivatives, $\partial^2 k/\partial \mathrm{N}_{\mathrm{mod}} \partial \Sigma$, for the infinite homogeneous problem 44

Table 3.7 Comparisons of the sensitivities of the reactivity coefficient of the coolant number density to the macroscopic cross sections of fuel-coolant mixture for the infinite homogeneous problem 45

Table 3.8 Two-group cross sections for the infinite homogeneous problem 46

Table 3.9 Comparisons of *k* sensitivities to the macroscopic cross sections, $\partial k/\partial \Sigma$, for the infinite homogeneous problem 47

Table 3.10 Comparisons of *k* sensitivities to the fuel temperature..... 48

Table 3.11 Comparisons of the second-order derivatives of *k* with respect to the fuel temperature and cross sections..... 50

Table 3.12 Comparisons of the second-order derivatives of *k* with respect to the fuel temperature and cross sections..... 51

Table 3.13 Comparisons of the sensitivities of the reactivity coefficient of fuel temperature to the macroscopic cross sections..... 52

Table 3.14 Comparisons of sensitivities of the ^{235}U-number-density coefficient to ^{235}U nuclear data for Godiva..... 55

Table 3.15 Comparisons of sensitivities of the ^{235}U-number-density coefficient to ^{238}U nuclear data for Godiva..... 56

Table 4.1 MDC uncertainties, $\sigma\left[\partial\rho/\partial D_M; X, X'\right]$, due to the covariance in ^{235}U and ^{238}U ENDF/B-VII.1 for the TMI-1 pin cell problem..... 60

Table 4.2 FTC uncertainties, $\sigma\left[\partial\rho/\partial T_f; X, X'\right]$, due to the covariance in ^{235}U and ^{238}U ENDF/B-VII.1 for the CANDU 6 lattice cell problem..... 62

List of Figures

Figure 3.1 Standard CANDU 6 Bundle problem..... 36

Chapter 1. Introduction

1.1 Background

Reactivity coefficients such as the fuel temperature coefficient (FTC) and the moderator density coefficient (MDC) of a nuclear reactor are important reactor physics parameters to assess its safety and maintain its safe operation. An accurate estimation of the reactivity coefficient is crucial especially when its value is close to zero like the FTC in the equilibrium core of CANDU 6 [1, 2]. For the accurate estimation, the direct subtraction method [2] or the perturbation method [3, 4] can be applied in the Monte Carlo (MC) neutron transport calculations with continuous-energy cross section libraries and a detailed geometry model. In the MC direct subtraction approach, the reactivity coefficient is calculated by subtracting reactivities obtained at a nominal state and a perturbed state. This direct subtraction method can be inefficient and even impossible to estimate the reactivity coefficient in some cases. For small perturbations, the relative error of the difference of two independent simulations can be much larger than the relative error of the nominal and perturbed reactivity. On the contrary to MC direct subtraction approach, the MC perturbation method is less time-consuming and as accurate at predicting the reactivity coefficient. The MC perturbation methods were demonstrated to estimate the density coefficients [5-8] and the FTC [9] with great efficiency.

The early MC perturbation method had been introduced with two perturbation techniques, now well-known correlated sampling (CS) and differential operator sampling (DOS) techniques. H. Rief generalized both techniques, giving their application results for estimating the coolant density coefficient in D_2O test reactor [3]. However, these early CS and DOS techniques were limited to consider only perturbation effect of response function, which means that they couldn't account for the perturbed source effect. Nagaya and Mori made the improvement of the conventional perturbation technique by including the fission source perturbation technique (FSP) to consider the effect of the perturbed fission source [4]. They demonstrated that FSP improves significantly the accuracy of MC perturbation calculations. On the other hand, the different approach to address the issue for the perturbed source effect had been suggested with an adjoint functions, which can be utilized to eliminate the perturbed source effect [7, 8]. Kiedrowdki and Brown proposed their approach to estimate the adjoint flux for kinetics parameters and reactivity change based on the iterated fission probability method [8]. Shim and Kim presented the similar MC adjoint-weighted perturbation (AWP) method applied to sensitivity and uncertainty analysis [7]. They demonstrated that the first-order AWP method is equivalent to the first-order DOS method with FSP. Later, they extended AWP method to estimate the FTC and presented its efficiency [9].

As mentioned above, the reactivity coefficient is the important parameter of

the safety operation and maintenance of the reactor and its uncertainty should be accurately estimated for the safety margin evaluation. There are two approaches to quantify the uncertainty of a nuclear performance parameter. One is the stochastic sampling method or Brute force method and another is the sensitivity and uncertainty analysis (S/U) based on the perturbation method [10]. Because of the input data uncertainties, there can be an infinitely different set of inputs. This may result in different outputs as many as the number of input sets. Then the variance of outputs can be estimated. This methodology is called the stochastic sampling method. This method is straightforward and free of any approximations but is expensive to produce large amount set of outputs for a sufficient statistical process. The uncertainty of the sodium void reactivity due to the nuclear covariance data has been calculated [11] by the stochastic sampling method named "Total Monte Carlo". On the other hands, when one can estimate the sensitivities of the design parameters with respect to input parameters, the uncertainties of design parameters can be obtained by multiplying the uncertainties of input parameters to the sensitivities. This is the S/U method and has pros to estimate the uncertainties efficiently. However, it is difficult to implement the perturbation modules to get the sensitivities. The reactivity coefficient is defined as the first-order derivative of the reactivity and its sensitivity can be at least express as the second-order derivative. Hence, there are difficulties to extend the first-order perturbation method to high order to estimate the sensitivities of reactivity coefficients.

M. L. Williams developed a sensitivity and uncertainty (S/U) analysis method for the reactivity difference based on the first-order perturbation method [12]. In this method (referred to as Williams' method hereafter), sensitivities of the reactivity coefficients with respect to the cross sections are expressed with the first-order k sensitivities at the two different states which are obtained by the MC perturbation techniques from two independent MC runs. Williams' method was applied to evaluate the uncertainty of the CANDU coolant void reactivity (CVR) due to the nuclear data uncertainties. Williams' method is effective for a large perturbation problem such as the CVR uncertainty quantification while it requires large amount of neutron history simulations to accurately estimate sensitivity of the reactivity coefficients such as FTC. Therefore, it is highly desirable to devise an alternative method to estimate the sensitivities of reactivity coefficients accurately and efficiently.

1.2 Objective

Objectives of this paper are to develop an alternative MC method to estimate the sensitivity of the reactivity coefficient to a cross section from a single MC run by applying second-order eigenvalue perturbation techniques [3, 13] and to apply the developed method for the uncertainty quantification of the reactivity coefficient. Rief [3] developed earlier the second-order

DOS method by taking into account second-order derivatives of the transport kernels and Morillon [14] extended it to an arbitrary order perturbation estimation. Recently Nagaya and Mori [13] devised a FSP algorithm to calculate higher-order terms of the perturbed source effect (PSE) which can be incorporated with the conventional DOS method to improve the accuracy of MC perturbation estimations. In Chapter 2, the new sensitivity calculation algorithm for the reactivity coefficient is derived by extending the existing second-order DOS [3] and FSP [13] methods into eigenvalue sensitivities to two different variables. The proposed MC second-order perturbation (MC2P) method is implemented in the Seoul National university Monte Carlo (MC) code, McCARD [15] and tested in a two-group homogeneous infinite medium problem by comparing MC2P results with analytic solutions. Its calculation efficiency is examined for the density coefficient of Godiva [16] by comparing with the Williams' method. In addition, the proposed method is applied to quantify the uncertainties of the MDC of a LWR pin cell problem and the FTC of a CANDU 6 lattice cell model [17] due to the nuclear covariance data.

Chapter 2. Monte Carlo Second-Order Perturbation Method for Sensitivity Estimation of Reactivity Coefficient

2.1. Derivation

The MC eigenvalue calculation with the fission source density (FSD), S, for a nuclear system is governed by

$$S = \frac{1}{k}\mathbf{H}S, \tag{2.1}$$

where k is the multiplication factor. $\mathbf{H}$ denotes the fission operator defined by

$$\mathbf{H}S = \int d\mathbf{P}' H\left(\mathbf{P}' \to \mathbf{P}\right) S\left(\mathbf{P}'\right); \tag{2.2}$$

$\mathbf{P}$ and $\mathbf{P}'$ denote state vectors of a neutron in the six-dimensional phase space, $(\mathbf{r},E,\mathbf{\Omega})$ and $(\mathbf{r}',E',\mathbf{\Omega}')$, respectively. $H(\mathbf{P} \to \mathbf{P}')$ means the number of first-generation fission neutrons born per unit phase space volume about $\mathbf{P}$, due to a parent neutron born at $\mathbf{P}'$, which can be explicitly expressed in terms of transport kernels as

$$H\left(\mathbf{P}' \to \mathbf{P}\right)\cdot = \sum_{j=0}^{\infty}\int dE''\int d\mathbf{\Omega}' C_f\left(\mathbf{r};E'',\mathbf{\Omega}' \to E,\mathbf{\Omega}\right)\int d\mathbf{r}_0 K_{s,j}\left(\mathbf{r}_0,E',\mathbf{\Omega}' \to \mathbf{r},E'',\mathbf{\Omega}'\right)T\left(E',\mathbf{\Omega}';\mathbf{r}' \to \mathbf{r}_0\right)\cdot, \tag{2.3}$$

where the fission collision kernel, C_f is defined by

$$C_f\left(\mathbf{r};E'',\mathbf{\Omega}''\to E,\mathbf{\Omega}\right)=\frac{\chi\left(E''\to E\right)}{4\pi}\cdot\frac{\nu\left(E''\right)\Sigma_f\left(\mathbf{r},E''\right)}{\Sigma_t\left(\mathbf{r},E''\right)} \tag{2.4}$$

ν is the mean number of fission neutrons produced from a fission reaction and χ is the energy spectrum of the fission neutron. $K_{s,p}$ is the p-th scattering kernel defined by

$$\begin{aligned} K_{s,0}\left(\mathbf{P}_0\to\mathbf{P}\right)&=\delta\left(\mathbf{P}_0\to\mathbf{P}\right),\\ K_{s,1}\left(\mathbf{P}_0\to\mathbf{P}\right)&=K_s\left(\mathbf{P}_0\to\mathbf{P}\right),\\ K_{s,p}\left(\mathbf{P}_0\to\mathbf{P}\right)&=\int d\mathbf{P}_{p-1}\cdots\int d\mathbf{P}_1 K_s\left(\mathbf{P}_{p-1}\to\mathbf{P}\right)\cdots K_s\left(\mathbf{P}_0\to\mathbf{P}_1\right);\ p=2,3,\cdots, \end{aligned} \tag{2.5}$$

where $\mathbf{P}_p$ (p=0,1,…) denote ($\mathbf{r}_p$,E_p,$\mathbf{\Omega}_p$) in $E_0 \equiv E'$ and $\mathbf{\Omega}_0 \equiv \mathbf{\Omega}'$. K_s is the transition kernel defined by the product of the scattering collision kernel, C_s, and the free flight kernel, T, as follows:

$$K_s\left(\mathbf{P}'\to\mathbf{P}\right)=T\left(E,\mathbf{\Omega};\mathbf{r}'\to\mathbf{r}\right)\cdot C_s\left(\mathbf{r}';E',\mathbf{\Omega}'\to E,\mathbf{\Omega}\right); \tag{2.6}$$

$$T\left(E,\mathbf{\Omega};\mathbf{r}'\to\mathbf{r}\right)=\frac{\Sigma_t\left(\mathbf{r},E\right)}{\left|\mathbf{r}-\mathbf{r}'\right|^2}\exp\left[-\int_0^{|\mathbf{r}-\mathbf{r}'|}\Sigma_t\left(\mathbf{r}-s\frac{\mathbf{r}-\mathbf{r}'}{\left|\mathbf{r}-\mathbf{r}'\right|},E\right)ds\right]\delta\left(\mathbf{\Omega}\cdot\frac{\mathbf{r}-\mathbf{r}'}{\left|\mathbf{r}-\mathbf{r}'\right|}-1\right), \tag{2.7}$$

$$C_s\left(\mathbf{r}';E',\mathbf{\Omega}'\to E,\mathbf{\Omega}\right)=\sum_{r\neq fis.}\nu_r\frac{\Sigma_r\left(\mathbf{r}';E',\mathbf{\Omega}'\right)}{\Sigma_t\left(\mathbf{r}',E'\right)}f_r\left(E',\mathbf{\Omega}'\to E,\mathbf{\Omega}\right). \tag{2.8}$$

ν_r is the average number of neutrons produced from a reaction type r and $f_r(E',\mathbf{\Omega}'\to E,\mathbf{\Omega})dEd\mathbf{\Omega}$ is the probability that a collision of type r by a neutron of direction $\mathbf{\Omega}'$ and energy E' will produce a neutron in direction interval $d\mathbf{\Omega}$ about $\mathbf{\Omega}$ with energy in dE about E. The k eigenvalue in Eq. (2.1) is estimated by scoring the number of next-generation fission neutrons in MC

neutron tracking starting from sources sampled from the FSD S, satisfying $\int S(\mathbf{P})d\mathbf{P} = 1$,

$$k = \langle \mathbf{H}S \rangle, \tag{2.9}$$

where the angular brackets <> imply an integration over the phase space **P**. When the static reactivity ρ of the nuclear system is defined by

$$\rho = 1 - \frac{1}{k}, \tag{2.10}$$

suppose that ρ is a function of two input parameters x and y representing a cross section and a physics parameter such as fuel temperature or coolant density, respectively, as $\rho \equiv \rho(x,y)$, i.e. $k \equiv k(x,y)$. Then by inserting Eq. (2.9) into Eq. (2.10) and taking a derivative of the resulting equation with respect to y, the reactivity coefficient of parameter y can be written as

$$\frac{\partial \rho}{\partial y} = \frac{1}{\langle \mathbf{H}S \rangle^2} \frac{\partial \langle \mathbf{H}S \rangle}{\partial y} = \frac{1}{\langle \mathbf{H}S \rangle^2} \left(\left\langle \frac{\partial \mathbf{H}}{\partial y} S \right\rangle + \left\langle \mathbf{H} \frac{\partial S}{\partial y} \right\rangle \right). \tag{2.11}$$

By taking a derivative of Eq. (2.11) with respect to x,

$$\frac{\partial^2 \rho}{\partial x \partial y} = -\frac{2}{k^3} \cdot \frac{\partial k}{\partial x} \cdot \frac{\partial k}{\partial y} + \frac{1}{k^2} \cdot \frac{\partial^2 k}{\partial x \partial y}; \tag{2.12}$$

$$\frac{\partial k}{\partial w} = \left\langle \frac{\partial \mathbf{H}}{\partial w} S \right\rangle + \left\langle \mathbf{H} \frac{\partial S}{\partial w} \right\rangle \quad (w = x \text{ or } y), \tag{2.13}$$

$$\frac{\partial^2 k}{\partial x \partial y} = \left\langle \frac{\partial^2 \mathbf{H}}{\partial x \partial y} S \right\rangle + \left\langle \frac{\partial \mathbf{H}}{\partial x} \cdot \frac{\partial S}{\partial y} \right\rangle + \left\langle \frac{\partial \mathbf{H}}{\partial y} \cdot \frac{\partial S}{\partial x} \right\rangle + \left\langle \mathbf{H} \frac{\partial^2 S}{\partial x \partial y} \right\rangle. \tag{2.14}$$

From Eq. (2.12), one can see that the sensitivity of the reactivity coefficient for y to x is calculated from k sensitivities of Eq. (2.13) and a second-order

derivative of k defined by Eq. (2.14). In Eq. (2.13), $\langle(\partial\mathbf{H}/\partial w)S\rangle$ is named the perturbed operator effect (POE) of the first-order k sensitivity while $\langle\mathbf{H}(\partial S/\partial w)\rangle$ is called the perturbed source effect (PSE). In Eq. (2.14), $\langle(\partial^2\mathbf{H}/\partial x\partial y)S\rangle$ and $\langle\mathbf{H}(\partial^2 S/\partial x\partial y)\rangle$ are the POE and PSE, respectively, of the second-order k sensitivity. The following sub-chapters describe how to calculate $\partial^2 k/\partial x\partial y$ by applying the MC perturbation techniques for the second-order terms in the RHS of Eq. (2.14) in the MC eigenvalue calculation.

2.2. First-Order DOS Method

In the MC power iteration method [18], the eigenvalue equation of Eq. (2.1) is solved cycle-by-cycle as

$$S_{i+1} = \frac{1}{k_i}\mathbf{H}S_i; \tag{2.15}$$

$$k_i = \langle\mathbf{H}S_i\rangle, \tag{2.16}$$

where i is the cycle index. $S_\ell(\ell = i \text{ or } i+1)$ is the FSD used for the cycle ℓ MC simulations and k_i is the eigenvalue estimate at cycle i. In order to calculate the term of $(\partial\mathbf{H}/\partial w)S$ in Eq. (2.13), one can take a derivative of the $\mathbf{H}$ operator defined by Eq. (2.3) with respect to parameter w (=x or y). The first-order DOS formulation for $(\partial\mathbf{H}/\partial w)S_i$ is obtained as

$$
\begin{aligned}
\frac{\partial \mathbf{H}}{\partial w} S_i &= \sum_{p=0}^{\infty} \int d\mathbf{P} \int dE'' \int d\mathbf{\Omega}'' \int d\mathbf{P}_{p-1} \cdots \int d\mathbf{P}_0 \int d\mathbf{r}' \\
&\quad \frac{\partial}{\partial w} \begin{pmatrix} C_{\mathrm{f}}\left(\mathbf{r}; E'', \mathbf{\Omega}'' \to E, \mathbf{\Omega}\right) K_s\left(\mathbf{P}_{p-1} \to \mathbf{r}, E'', \mathbf{\Omega}''\right) \\ \cdots K_S\left(\mathbf{P}_0 \to \mathbf{P}_1\right) T\left(E_0, \mathbf{\Omega}_0; \mathbf{r}' \to \mathbf{r}_0\right) \end{pmatrix} S_i\left(\mathbf{r}', E_0, \mathbf{\Omega}_0\right) \\
&= \sum_{p=0}^{\infty} \int d\mathbf{P} \int dE'' \int d\mathbf{\Omega}'' \int d\mathbf{P}_{p-1} \cdots \int d\mathbf{P}_0 \int d\mathbf{r}' \, U_w^{\mathbf{H}} \\
&\quad \cdot \begin{Bmatrix} C_{\mathrm{f}}\left(\mathbf{r}; E'', \mathbf{\Omega}'' \to E, \mathbf{\Omega}\right) K_s\left(\mathbf{P}_{p-1} \to \mathbf{r}, E'', \mathbf{\Omega}''\right) \\ \cdots K_S\left(\mathbf{P}_0 \to \mathbf{P}_1\right) T\left(E_0, \mathbf{\Omega}_0; \mathbf{r}' \to \mathbf{r}_0\right) \end{Bmatrix} S_i\left(\mathbf{r}', E_0, \mathbf{\Omega}_0\right)
\end{aligned}
\tag{2.17}
$$

$U_w^{\mathbf{H}}$ of Eq. (2.17) can be shown with the sensitivity coefficients of the transport kernels with respect to parameter w as

$$
\begin{aligned}
U_w^{\mathbf{H}}(\mathbf{r}', E_0, \mathbf{\Omega}_0 \to \mathbf{P}) \equiv\, & u_w^f(\mathbf{r}; E'', \mathbf{\Omega}'' \to E, \mathbf{\Omega}) + u_w^K(\mathbf{P}_{p-1} \to \mathbf{r}, E'', \mathbf{\Omega}'') \\
& + \sum_{k=0}^{p-2} u_w^K(\mathbf{P}_p \to \mathbf{P}_{p+1}) + u_w^T(E_0, \mathbf{\Omega}_0; \mathbf{r}' \to \mathbf{r}_0),
\end{aligned}
\tag{2.18}
$$

where

$$
u_w^f(\mathbf{r}; E'', \mathbf{\Omega}'' \to E, \mathbf{\Omega}) \equiv \frac{1}{C_f(\mathbf{r}; E'', \mathbf{\Omega}'' \to E, \mathbf{\Omega})} \frac{\partial C_f(\mathbf{r}; E'', \mathbf{\Omega}'' \to E, \mathbf{\Omega})}{\partial w}, \tag{2.19}
$$

$$
\begin{aligned}
u_w^K(\mathbf{P}_p \to \mathbf{P}_{p+1}) &\equiv \frac{1}{K_s(\mathbf{P}_p \to \mathbf{P}_{p+1})} \frac{\partial K_s(\mathbf{P}_p \to \mathbf{P}_{p+1})}{\partial w}, \\
&\equiv u_w^T\left(E_{p+1}, \mathbf{\Omega}_{p+1}; \mathbf{r}_p \to \mathbf{r}_{p+1}\right) + u_w^C\left(\mathbf{r}_p; E_p, \mathbf{\Omega}_p \to E_{p+1}, \mathbf{\Omega}_{p+1}\right)
\end{aligned}
\tag{2.20}
$$

$$
\begin{aligned}
& u_w^C\left(\mathbf{r}_p; E_p, \mathbf{\Omega}_p \to E_{p+1}, \mathbf{\Omega}_{p+1}\right) \\
& \equiv \frac{1}{C_s\left(\mathbf{r}_p; E_p, \mathbf{\Omega}_p \to E_{p+1}, \mathbf{\Omega}_{p+1}\right)} \frac{\partial C_s\left(\mathbf{r}_p; E_p, \mathbf{\Omega}_p \to E_{p+1}, \mathbf{\Omega}_{p+1}\right)}{\partial w}
\end{aligned}
\tag{2.21}
$$

$$u_w^T(E_{p+1},\mathbf{\Omega}_{p+1};\mathbf{r}_p \to \mathbf{r}_{p+1}) \equiv \frac{1}{T(E_{p+1},\mathbf{\Omega}_{p+1};\mathbf{r}_p \to \mathbf{r}_{p+1})} \frac{\partial T(E_{p+1},\mathbf{\Omega}_{p+1};\mathbf{r}_p \to \mathbf{r}_{p+1})}{\partial w}. \tag{2.22}$$

In MC random walk process, the *p*-th track starts with a neutron undergoing reaction type "a" with isotope i' at energy $E_{p\text{-}1}$ and $\mathbf{\Omega}_{p\text{-}1}$ is scattered to E_p and $\mathbf{\Omega}_p$ and continues for track length λ_p and collides, the sampled scattering collision kernel and the sampled free flight kernel can be written as

$$\begin{aligned} C_{s,p} &\equiv C_s\left(\mathbf{r}_{p-1};E_{p-1},\mathbf{\Omega}_{p-1} \to E_p,\mathbf{\Omega}_p\right) \\ &= \nu_\alpha^{i'} \frac{N^{i'}\left(E_{p-1}\right)}{\Sigma_t\left(E_{p-1}\right)} f_\alpha^{i'}\left(E_{p-1}\mathbf{\Omega}_{p-1} \to E_p,\mathbf{\Omega}_p\right), \end{aligned} \tag{2.23}$$

$$T_p \equiv T\left(E_p,\mathbf{\Omega}_p;\mathbf{r}_{p-1} \to \mathbf{r}_p\right) = \frac{\Sigma_t\left(E_p\right)}{\lambda_p^2} \exp\left[-\Sigma_t\left(E_p\right)\lambda_p\right]. \tag{2.24}$$

Using Eqs. (2.23) and (2.24), the first-order sensitivity coefficient of transport kernel of Eq. (2.20) for the *p*-th track can be calculated by

$$u_{w,p}^K = \begin{cases} \dfrac{1}{C_{s,p}} \dfrac{\partial C_{s,p}}{\partial w} + \dfrac{1}{T_p} \dfrac{\partial T_p}{\partial w} & \left(p = 1,2,\cdots\right) \\ \dfrac{1}{T_p} \dfrac{\partial T_p}{\partial w} \end{cases}. \tag{2.25}$$

The first-order sensitivity coefficient of transport kernel to the α-type cross section of *i* isotope can be calculated using

$$\begin{aligned}\frac{1}{C_{s,p}}\frac{\partial C_{s,p}}{\partial\alpha}&=\frac{1}{v_\alpha^{i'}\dfrac{N^{i'}\sigma_a^{i'}\left(E_{p-1}\right)}{\Sigma_t\left(E_{p-1}\right)}f_a^{i'}\left(E_{p-1},\mathbf{\Omega}_{p-1}\to E_p,\mathbf{\Omega}_p\right)}\\&\cdot\begin{pmatrix}v_\alpha^{i'}\dfrac{N^{i'}\delta_{ii'}\delta_{a\gamma}}{\Sigma_t\left(E_{p-1}\right)}f_a^{i'}\left(E_{p-1},\mathbf{\Omega}_{p-1}\to E_p,\mathbf{\Omega}_p\right)\\-v_\alpha^{i'}N^i\dfrac{N^{i'}\sigma_a^{i'}\left(E_{p-1}\right)}{\Sigma_t\left(E_{p-1}\right)^2}f_a^{i'}\left(E_{p-1},\mathbf{\Omega}_{p-1}\to E_p,\mathbf{\Omega}_p\right)\end{pmatrix}\\&=\frac{1}{\sigma_a^i\left(E_{p-1}\right)}\delta_{ii'}\delta_{a\alpha}-\frac{N^i}{\Sigma_t\left(E_{p-1}\right)},\end{aligned}\tag{2.26}$$

$$\begin{aligned}\frac{1}{T_p}\frac{\partial T_p}{\partial\alpha}&=\frac{1}{\dfrac{\Sigma_t\left(E_p\right)}{\lambda_p^2}\exp\left[-\Sigma_t\left(E_p\right)\lambda_p\right]}\begin{pmatrix}\dfrac{N^i}{\lambda_p^2}\exp\left[-\Sigma_t\left(E_p\right)\lambda_p\right]\\-\lambda_pN^i\dfrac{\Sigma_t\left(E_p\right)}{\lambda_p^2}\exp\left[-\Sigma_t\left(E_p\right)\lambda_p\right]\end{pmatrix}\\&=\frac{N^i}{\Sigma_t\left(E_p\right)}-\lambda_pN^i.\end{aligned}\tag{2.27}$$

For a $C_f\left(\mathbf{P}\right)\left(=\nu\Sigma_f/\Sigma_t\right)$ which denotes a response function for the collision estimator of *k*, the first-order sensitivity coefficient $u_{w,p}^f$ from the *p*-th track can be calculated by

$$u_{\alpha,p}^f=\frac{\Sigma_t\left(\mathbf{r}_p,E_p\right)}{\nu_f\left(\mathbf{r}_p,E_p\right)\Sigma_f\left(\mathbf{r}_p,E_p\right)}\frac{\partial}{\partial\alpha}\left(\frac{\nu_f\left(\mathbf{r}_p,E_p\right)\Sigma_f\left(\mathbf{r}_p,E_p\right)}{\Sigma_t\left(\mathbf{r}_p,E_p\right)}\right).\tag{2.28}$$

The first-order sensitivity of $C_f\left(\mathbf{P}\right)$ to the α-type cross section of *i* isotope, can be calculated using

$$u_{\alpha,p}^{f}=\frac{\nu^{i}\left(\mathbf{r}_{p},E_{p}\right)N^{i}}{\nu\left(\mathbf{r}_{p},E_{p}\right)\Sigma_{f}\left(\mathbf{r}_{p},E_{p}\right)}\delta_{af}-\frac{N^{i}}{\Sigma_{t}\left(\mathbf{r}_{p},E_{p}\right)} \tag{2.29}$$

or if α-type cross section denotes nu value, the sensitivity can be calculated using

$$u_{\nu_{f},p}^{f}=\frac{\Sigma_{f}^{i}\left(\mathbf{r}_{p},E_{p}\right)}{\nu_{f}\left(\mathbf{r}_{p},E_{p}\right)\Sigma_{f}\left(\mathbf{r}_{p},E_{p}\right)} \tag{2.30}$$

2.3. First-Order FSP Method

In the first-order FSP method, the sensitivity coefficient of S_i to parameter w, $u_{w}^{S_i}$, is calculated by differentiating Eq. (2.15) and dividing the resulting equation with the FSD, S_i. Then the first-order sensitivity coefficient of S_i can be obtained by

$$\begin{aligned} u_{w}^{S_i}&=\frac{1}{S_i}\frac{\partial S_i}{\partial w}=\frac{1}{k_{i-1}\cdot S_i}\frac{\partial}{\partial w}\left[\mathbf{H}S_{i-1}\right]-\frac{1}{k_{i-1}^{2}\cdot S_i}\frac{\partial k_{i-1}}{\partial w}\mathbf{H}S_{i-1} \\ &=\frac{1}{k_{i-1}\cdot S_i}\frac{\partial}{\partial w}\left[\mathbf{H}S_{i-1}\right]-\frac{1}{k_{i-1}}\frac{\partial k_{i-1}}{\partial w}. \end{aligned} \tag{2.31}$$

Using Eq. (2.16), the second term in RHS of Eq. (2.31) can be written as

$$\frac{1}{k_{i-1}}\frac{\partial k_{i-1}}{\partial w}=\frac{\left\langle \frac{\partial}{\partial w}\left[\mathbf{H}\mathrm{S}_{i-1}\right]\right\rangle}{\left\langle \mathbf{H}\mathrm{S}_{i-1}\right\rangle} \tag{2.32}$$

By inserting Eqs. (2.2) and (2.3) into Eq. (2.31), the first term in RHS of Eq. (2.31) can be written with explicit kernels as

$$\frac{1}{k_{i-1}\cdot S_i}\frac{\partial}{\partial w}\left[\mathbf{H}S_{i-1}\right]=\frac{1}{k_{i-1}\cdot S_i(\mathbf{P})}\cdot\left\{\begin{array}{l}\displaystyle\sum_{p=0}^{\infty}\int dE''\int d\mathbf{\Omega}''\int d\mathbf{P}_{p-1}\cdots\int d\mathbf{P}_0\int d\mathbf{r}' \\ \cdot\left[U_w^{\mathbf{H}}(\mathbf{r}',E_0,\mathbf{\Omega}_0\to\mathbf{P})+u_w^{S_{i-1}}(\mathbf{r}',E_0,\mathbf{\Omega}_0)\right] \\ \cdot C_{\mathrm{f}}(\mathbf{r};E'',\mathbf{\Omega}''\to E,\mathbf{\Omega})K_s(\mathbf{P}_{p-1}\to\mathbf{r},E'',\mathbf{\Omega}'') \\ \cdots K_S(\mathbf{P}_0\to\mathbf{P}_1)T(E_0,\mathbf{\Omega}_0;\mathbf{r}'\to\mathbf{r}_0)S_{i-1}(\mathbf{r}',E_0,\mathbf{\Omega}_0)\end{array}\right\}. \quad (2.33)$$

In the MC random work simulation, Eq. (2.33) can be estimated by calculating the values of $U^{\mathbf{H}}_{w,(i-1)j'p}$ and $u_w^{S(i-1)j'}$. The sum of the values of $U^{\mathbf{H}}_{w,(i-1)j'p}$ and $u_w^{S(i-1)j'}$ can be defined with $U^{\mathbf{H}S}_{w,(i-1)j'p}$ as

$$U^{\mathbf{H}S}_{w,(i-1)j'p}\equiv\left(\frac{1}{k_{i-1}\cdot S_i}\frac{\partial}{\partial w}\left[\mathbf{H}S_{i-1}\right]\right)_{j'p}=U^{\mathbf{H}}_{w,(i-1)j'p}+u_w^{S_{(i-1)j'}}. \quad (2.34)$$

where $(\cdot)_{j'p}$ means an MC estimate of an inside variable from collision p of history j'. $U^{\mathbf{H}}_{w,(i-1)j'p}$ denotes the values of $U^{\mathbf{H}}_{w,(i-1)}$ in Eq. (2.18) at the p-th collision site of j'-th history from which fission source neutron generated for the next cycle. $u_w^{S(i-1)j'}$ denotes the first-order sensitivity coefficient of $S_{i\text{-}1}$ of the j'-th source at cycle i-1, $S_{(i=1)j'}$. Using Eq. (2.16), Eq. (2.32) can be written with explicit transport kernels as

$$\frac{\left\langle \frac{\partial}{\partial w}\left[\mathbf{HS}_{i-1}\right]\right\rangle}{\left\langle \mathbf{HS}_{i-1}\right\rangle}=\frac{\begin{array}{l}\sum_{p=0}^{\infty}\int d\mathbf{P}\int dE''\int d\mathbf{\Omega}''\int d\mathbf{P}_{p-1}\cdots\int d\mathbf{P}_0\int d\mathbf{r}' \\ \cdot\left\{\begin{array}{l}\left[U_w^{\mathbf{H}}\left(\mathbf{r}',E_0,\mathbf{\Omega}_0\to\mathbf{P}\right)+u_w^{S_{i-1}}\left(\mathbf{r}',E_0,\mathbf{\Omega}_0\right)\right] \\ \cdot C_{\mathrm{f}}\left(\mathbf{r};E'',\mathbf{\Omega}''\to E,\mathbf{\Omega}\right)K_s\left(\mathbf{P}_{p-1}\to\mathbf{r},E'',\mathbf{\Omega}''\right)\cdots \\ \cdot K_S\left(\mathbf{P}_0\to\mathbf{P}_1\right)T\left(E_0,\mathbf{\Omega}_0;\mathbf{r}'\to\mathbf{r}_0\right)S_{i-1}\left(\mathbf{r}',E_0,\mathbf{\Omega}_0\right)\end{array}\right\}\end{array}}{\begin{array}{l}\sum_{p=0}^{\infty}\int d\mathbf{P}\int dE''\int d\mathbf{\Omega}''\int d\mathbf{P}_{p-1}\cdots\int d\mathbf{P}_0\int d\mathbf{r}' \\ \cdot\left\{\begin{array}{l}C_{\mathrm{f}}\left(\mathbf{r};E'',\mathbf{\Omega}''\to E,\mathbf{\Omega}\right)K_s\left(\mathbf{P}_{p-1}\to\mathbf{r},E'',\mathbf{\Omega}''\right)\cdots \\ \cdot K_S\left(\mathbf{P}_0\to\mathbf{P}_1\right)T\left(E_0,\mathbf{\Omega}_0;\mathbf{r}'\to\mathbf{r}_0\right)S_{i-1}\left(\mathbf{r}',E_0,\mathbf{\Omega}_0\right)\end{array}\right\}\end{array}}. \quad (2.35)$$

In the same way to derive the MC algorithm of Eq. (2.34) from Eq. (2.33), Eq. (2.35) can be estimated by

$$\begin{aligned}U_{w,(i-1)}^{k}&\equiv\left(\frac{1}{k_{i-1}}\cdot\frac{\partial k_{i-1}}{\partial w}\right)_{\forall j'}=\left(\frac{1}{\left\langle \mathbf{HS}_{i-1}\right\rangle}\left\langle \frac{\partial}{\partial w}\left[\mathbf{HS}_{i-1}\right]\right\rangle\right)_{\forall j'} \\ &=\frac{\sum_{j'}\sum_{p}U_{w,(i-1)j'p}^{\mathbf{HS}}\cancel{k_{i-1}}n_{f,(i-1)j'p}}{\sum_{j'}\sum_{p}\cancel{k_{i-1}}n_{f,(i-1)j'p}} \\ &=\frac{\sum_{j'}\sum_{p}U_{w,(i-1)j'p}^{\mathbf{HS}}n_{f,(i-1)j'p}}{\sum_{j'}\sum_{p}n_{f,(i-1)j'p}}\end{aligned} \quad (2.36)$$

where $n_{f,(i-1)j'p}$ is the number of fission sources generated by p-th collision of j'-th history at cycle (i-1). The first-order sensitivity coefficient of S_{ij}, $u_w^{S_{ij}}$, can be estimated by inserting Eqs. (2.34) and Eq. (2.36) into Eq. (2.31) as

$$u_w^{S_{ij}}=U_{w,(i-1)j'p}^{\mathbf{HS}}-U_{w,(i-1)}^{k}\cdot\cdot \quad (2.37)$$

By assuming $u_w^{S_{(i-n)}}$ to be zero where n is called the propagation batch size

[6], the first-order sensitivity coefficient $u_w^{S_{ij}}$ can be obtained recursively in the iteration process.

2.4. Second-Order DOS Method for Two Variables

In order to calculate the term of $\left\langle \left(\partial^2 \mathbf{H}/\partial x \partial y\right) S \right\rangle$ in Eq. (2.14), one can take a derivative of the **H** operator defined by Eqs. (2.2) and (2.3) with respect to x and y, the second-order DOS formulation for $\left(\partial^2 \mathbf{H}/\partial x \partial y\right) S_i$ is obtained as

$$\left\langle \frac{\partial^2 \mathbf{H}}{\partial x \partial y} S_i \right\rangle = \sum_{p=0}^{\infty} \int d\mathbf{P} \int dE'' \int d\mathbf{\Omega}'' \int d\mathbf{P}_{p-1} \cdots \int d\mathbf{P}_0 \int d\mathbf{r}' \, U_{xy}^{\mathbf{H}} + U_x^{\mathbf{H}} U_y^{\mathbf{H}} \cdot \begin{Bmatrix} C_f\left(\mathbf{r}; E'', \mathbf{\Omega}'' \to E, \mathbf{\Omega}\right) K_s\left(\mathbf{P}_{p-1} \to \mathbf{r}, E'', \mathbf{\Omega}''\right) \cdots \\ \cdot K_s\left(\mathbf{P}_0 \to \mathbf{P}_1\right) T\left(E_0, \mathbf{\Omega}_0; \mathbf{r}' \to \mathbf{r}_0\right) \end{Bmatrix} S_i\left(\mathbf{r}', E_0, \mathbf{\Omega}_0\right) \tag{2.38}$$

$U_{xy}^{\mathbf{H}}$ in Eq. (2.38) can be shown with the second-order and first-order sensitivity coefficient of the transport kernels with respect to parameter x and y as

$$U_{xy}^{\mathbf{H}}(\mathbf{r}', E_0, \mathbf{\Omega}_0 \to \mathbf{P}) \equiv u_{xy}^{f}(\mathbf{r}; E'', \mathbf{\Omega}'' \to E, \mathbf{\Omega}) + u_{xy}^{K}(\mathbf{P}_{p-1} \to \mathbf{r}, E'', \mathbf{\Omega}'') + \sum_{k=0}^{p-2} u_{xy}^{K}(\mathbf{P}_p \to \mathbf{P}_{p+1}) + u_{xy}^{T}(E_0, \mathbf{\Omega}_0; \mathbf{r}' \to \mathbf{r}_0), \tag{2.39}$$

where

$$u_{xy}^{f}(\mathbf{r}; E'', \mathbf{\Omega}'' \to E, \mathbf{\Omega}) \equiv u_x^{f}(\mathbf{r}; E'', \mathbf{\Omega}'' \to E, \mathbf{\Omega}) \cdot u_y^{f}(\mathbf{r}; E'', \mathbf{\Omega}'' \to E, \mathbf{\Omega}) + \frac{1}{C_f(\mathbf{r}; E'', \mathbf{\Omega}'' \to E, \mathbf{\Omega})} \frac{\partial^2 C_f(\mathbf{r}; E'', \mathbf{\Omega}'' \to E, \mathbf{\Omega})}{\partial x \partial y}, \tag{2.40}$$

$$u_{xy}^{K}(\mathbf{P}_p \to \mathbf{P}_{p+1}) \equiv u_{xy}^{T}(E_{p+1},\mathbf{\Omega}_{p+1};\mathbf{r}_p \to \mathbf{r}_{p+1}) + u_{xy}^{C}(\mathbf{r}_p;E_p,\mathbf{\Omega}_p \to E_{p+1},\mathbf{\Omega}_{p+1}), \quad (2.41)$$

$$\begin{aligned} & u_{xy}^{C}(\mathbf{r}_p;E_p,\mathbf{\Omega}_p \to E_{p+1},\mathbf{\Omega}_{p+1}) \\ & \equiv -u_{x}^{C}(\mathbf{r}_p;E_p,\mathbf{\Omega}_p \to E_{p+1},\mathbf{\Omega}_{p+1})u_{y}^{C}(\mathbf{r}_p;E_p,\mathbf{\Omega}_p \to E_{p+1},\mathbf{\Omega}_{p+1}) \\ & \quad + \frac{1}{C_s(\mathbf{r}_p;E_p,\mathbf{\Omega}_p \to E_{p+1},\mathbf{\Omega}_{p+1})} \frac{\partial^2 C(\mathbf{r}_p;E_p,\mathbf{\Omega}_p \to E_{p+1},\mathbf{\Omega}_{p+1})}{\partial x \partial y} \end{aligned} \quad (2.42)$$

$$\begin{aligned} u_{xy}^{T}(E_{p+1},\mathbf{\Omega}_{p+1};\mathbf{r}_p \to \mathbf{r}_{p+1}) \equiv & -u_{x}^{T}(E_{p+1},\mathbf{\Omega}_{p+1};\mathbf{r}_p \to \mathbf{r}_{p+1})u_{y}^{T}(E_{p+1},\mathbf{\Omega}_{p+1};\mathbf{r}_p \to \mathbf{r}_{p+1}) \\ & + \frac{1}{T(E_{p+1},\mathbf{\Omega}_{p+1};\mathbf{r}_p \to \mathbf{r}_{p+1})} \frac{\partial^2 T(E_{p+1},\mathbf{\Omega}_{p+1};\mathbf{r}_p \to \mathbf{r}_{p+1})}{\partial x \partial y}, \end{aligned} \quad (2.43)$$

If y is a number density of isotope "j" and x is α-type cross section of i isotope, the second-order sensitivity coefficient, u_{xy}^{f} can be calculated in the MC simulation by

$$u_{xy,p}^{f} = \frac{\partial u_{y,p}^{f}}{\partial x} = \frac{\partial}{\partial x}\left(\frac{\Sigma_t(\mathbf{r}_p,E_p)}{\nu_f(\mathbf{r}_p,E_p)\Sigma_f(\mathbf{r}_p,E_p)} \frac{\partial}{\partial y}\left(\frac{\nu_f(\mathbf{r}_p,E_p)\Sigma_f(\mathbf{r}_p,E_p)}{\Sigma_t(\mathbf{r}_p,E_p)} \right) \right). \quad (2.44)$$

If x is a fission reaction cross section of i isotope, Eq. (2.44) can be calculated using

$$\begin{aligned} \frac{\partial u_{y,p}^{f}}{\partial x} = \frac{\partial u_{y,p}^{f}}{\partial x} = & \frac{\nu^i(\mathbf{r}_p,E_p)}{\nu(\mathbf{r}_p,E_p)\Sigma_f(\mathbf{r}_p,E_p)}\delta_{ij} - \frac{\nu^i(\mathbf{r}_p,E_p)\mathrm{N}^j}{\nu(\mathbf{r}_p,E_p)\Sigma_f(\mathbf{r}_p,E_p)} \cdot \frac{\nu^j(\mathbf{r}_p,E_p)\sigma_f^j(\mathbf{r}_p,E_p)}{\nu(\mathbf{r}_p,E_p)\Sigma_f(\mathbf{r}_p,E_p)} \\ & - \frac{1}{\Sigma_t(\mathbf{r}_p,E_p)}\delta_{ij} + \frac{\mathrm{N}^i}{\Sigma_t(\mathbf{r}_p,E_p)} \frac{\sigma_t^j}{\Sigma_t(\mathbf{r}_p,E_p)} \end{aligned}$$

(2.45)

or if x is nu value of isotope i, Eq. (2.44) is

$$\frac{\partial u_{y,p}^{f}}{\partial x}=\frac{\nu^{i}\left(\mathbf{r}_{p},E_{p}\right)}{\nu\left(\mathbf{r}_{p},E_{p}\right)\Sigma_{f}\left(\mathbf{r}_{p},E_{p}\right)}\delta_{ij}-\frac{\nu^{i}\left(\mathbf{r}_{p},E_{p}\right)\mathrm{N}^{j}}{\nu\left(\mathbf{r}_{p},E_{p}\right)\Sigma_{f}\left(\mathbf{r}_{p},E_{p}\right)}\cdot\frac{\nu^{j}\left(\mathbf{r}_{p},E_{p}\right)\sigma_{f}^{j}\left(\mathbf{r}_{p},E_{p}\right)}{\nu\left(\mathbf{r}_{p},E_{p}\right)\Sigma_{f}\left(\mathbf{r}_{p},E_{p}\right)}. \tag{2.46}$$

In the case for the other type cross section, Eq. (2.44) is

$$\frac{\partial u_{y,p}^{f}}{\partial x}=-\frac{1}{\Sigma_{t}\left(\mathbf{r}_{p},E_{p}\right)}\delta_{ij}+\frac{\mathrm{N}^{i}}{\Sigma_{t}\left(\mathbf{r}_{p},E_{p}\right)}\frac{\sigma_{t}^{j}}{\Sigma_{t}\left(\mathbf{r}_{p},E_{p}\right)}. \tag{2.47}$$

The second-order sensitivity coefficient u_{xy}^{T} for the p-th track can be calculated by

$$\frac{\partial}{\partial x}\left[\frac{1}{T_{p}}\frac{\partial T_{p}}{\partial y}\right]=\left(-\lambda_{p}+\frac{1}{\Sigma_{t}\left(E_{p}\right)}\right)\delta_{ij}-\frac{\Sigma_{t}^{j}\left(E_{p}\right)\Sigma_{\alpha}^{i}\left(E_{p}\right)}{\Sigma_{t}\left(E_{p}\right)^{2}}\cdot\frac{1}{\sigma_{\alpha}^{i}\left(E_{p}\right)}\cdot\frac{1}{\mathrm{N}^{j}}. \tag{2.48}$$

The second-order sensitivity coefficient, u_{xy}^{C} for the p-th track can be calculated by

$$\frac{\partial}{\partial x}\left[\frac{1}{C_{s,p}}\frac{\partial C_{s,p}}{\partial y}\right]=-\frac{1}{\Sigma_{t}\left(E_{p}\right)}\delta_{ij}+\left(\frac{\Sigma_{t}^{j}\left(E_{p}\right)\Sigma_{\alpha}^{i}\left(E_{p}\right)}{\Sigma_{t}\left(E_{p}\right)^{2}}+\delta_{x\gamma}-\delta_{yj}\delta_{x\gamma}\right)\cdot\frac{1}{\sigma_{\alpha}^{i}\left(E_{p}\right)}\frac{1}{\mathrm{N}^{j}}. \tag{2.49}$$

Next, the analytic expressions for the second-order coefficient when y is the α'-type cross section of j-isotope are written as follows. The second-order sensitivity coefficient u_{xy}^{T} for the p-th track can be calculated by

$$u_{xy}^{T}=\frac{\partial}{\partial x}\left[\frac{1}{T_p}\frac{\partial T_p}{\partial y}\right]=\frac{\partial}{\partial x}\left[\frac{1}{\Sigma_t(E_p)}-\lambda_p\right]N^j$$
$$=\left[-\frac{1}{\Sigma_t(E_p)^2}\right]N^iN^j \tag{2.50}$$

The second-order sensitivity coefficient u_{xy}^{C} for the p-th track can be calculated by

$$u_{xy}^{C}=\frac{\partial}{\partial x}\left[\frac{1}{C_{s,p}}\frac{\partial C_{s,p}}{\partial y}\right]=\frac{\partial}{\partial x}\left[\frac{1}{\Sigma_{a'}^{j}(E_p)}\delta_{jj'}\delta_{a\alpha'}-\frac{1}{\Sigma_t(E_p)}\right]N^j$$
$$=\left[-\frac{1}{\Sigma_{a'}^{j}(E_p)^2}\delta_{ij}\delta_{a\alpha}\delta_{jj'}\delta_{a\alpha'}+\frac{1}{\Sigma_t(E_p)^2}\right]N^iN^j \tag{2.51}$$

The second-order sensitivity coefficient u_{xy}^{f} to fission reaction cross section of i isotope and a different type of cross section of j-isotope can be written by

$$u_{\sigma_f^i\nu_f^j}^{f}=\frac{\partial}{\partial\sigma_f^i}\left[\frac{\Sigma_f^j\left(E_p\right)}{\nu\left(E_p\right)\Sigma_f\left(E_p\right)}\right]=\left(-\frac{\Sigma_f^j\left(E_p\right)\nu^i\left(E_p\right)\mathrm{N}^i}{\nu\left(E_p\right)\Sigma_f\left(E_p\right)^2}+\frac{\mathrm{N}^i}{\nu\left(E_p\right)\Sigma_f\left(E_p\right)}\delta_{ij}\right) \tag{2.52}$$

$$u_{\sigma_f^i\sigma_f^j}^{f}=\frac{\partial}{\partial\sigma_f^i}\left[\frac{\nu^j\left(E_p\right)\mathrm{N}^j}{\nu\left(E_p\right)\Sigma_f\left(E_p\right)}-\frac{\mathrm{N}^j}{\Sigma_t\left(E_p\right)}\right]$$
$$=\left(-\frac{\nu^j\left(E_p\right)\mathrm{N}^j\cdot\nu^i\left(E_p\right)\mathrm{N}^i}{\nu\left(E_p\right)\Sigma_f\left(E_p\right)^2}+\frac{\mathrm{N}^j\mathrm{N}^i}{\Sigma_t\left(E_p\right)^2}\right) \tag{2.53}$$

$$u_{\sigma_f^i\sigma_\gamma^j}^{f}=\frac{\partial}{\partial\sigma_f^i}\left[-\frac{\mathrm{N}^j}{\Sigma_t\left(E_p\right)}\right]=\frac{\mathrm{N}^j\cdot\mathrm{N}^i}{\Sigma_t\left(E_p\right)^2} \tag{2.54}$$

y is nu value of *j*-isotope in Eq. (2.52), fission reaction cross section of *j*-isotope in Eq. (2.53), and the other α-type cross section in Eq. (2.54).

In the case for *x* is nu value of nuclide *i*, u_{xy}^{f} can be written by

$$\frac{\partial}{\partial \nu_f^i}\left[u_{\nu_f^j}^f\right]=\frac{\partial}{\partial \nu^i}\left[\frac{\Sigma_f^j\left(E_p\right)}{\nu\Sigma_f\left(E_p\right)}\right]=-\frac{\Sigma_f^j\left(E_p\right)\Sigma_f^i\left(E_p\right)}{\nu\left(E_p\right)\Sigma_f\left(E_p\right)^2} \tag{2.55}$$

$$\begin{aligned}\frac{\partial}{\partial \nu^i}\left[u_{\sigma_f^j}^f\right]&=\frac{\partial}{\partial \nu^i}\left[\frac{\nu^j\left(E_p\right)\mathrm{N}^j}{\nu\left(E_p\right)\Sigma_f\left(E_p\right)}-\frac{\mathrm{N}^j}{\Sigma_t\left(E_p\right)}\right]\\&=\left(-\frac{\nu^j\left(E_p\right)\mathrm{N}^j\cdot\Sigma_f^i\left(E_p\right)}{\nu\left(E_p\right)^2\Sigma_f\left(E_p\right)^2}+\frac{\mathrm{N}^j}{\nu\left(E_p\right)\Sigma_f\left(E_p\right)}\delta_{ij}\right)\end{aligned} \tag{2.56}$$

$$\frac{\partial}{\partial \nu^i}\left[u_{\sigma_\gamma^j}^f\right]=\frac{\partial}{\partial \nu^i}\left[-\frac{\mathrm{N}^j}{\Sigma_t\left(E_k\right)}\right]=0. \tag{2.57}$$

y is nu value of *j*-isotope in Eq. (2.55), fission reaction cross section of *j*-isotope in Eq. (2.56), and the other α-type cross section in Eq. (2.57).

In the case for *x* is the other type of cross sections of nuclide *i*, u_{xy}^{f} can be written by

$$u_{\sigma_\alpha^i\nu^j}^f=\frac{\partial}{\partial\sigma_\alpha^i}\left[\frac{\Sigma_f^j\left(E_p\right)}{\nu\left(E_p\right)\Sigma_f\left(E_p\right)}\right]=0 \tag{2.58}$$

$$u_{\sigma_a^i\sigma_f^j}^f=\frac{\mathrm{N}^j\mathrm{N}^i}{\Sigma_t\left(E_p\right)^2} \tag{2.59}$$

y is nu value of *j*-isotope in Eq. (2.58) and fission reaction cross section of *j*-isotope in Eq. (2.59).

2.5. Second-Order FSP Method for Two Variables

The terms of $(\partial\mathbf{H}/\partial x)\cdot(\partial S/\partial y)$ and $(\partial\mathbf{H}/\partial y)\cdot(\partial S/\partial x)$ in Eq. (2.14) represented by $(\partial\mathbf{H}/\partial w')\cdot(\partial S/\partial w)$ $((w',w)=(x,y)$ or $(y,x))$ can be calculated by taking a derivative of the **H** operator defined by Eq. (2.3) with respect to w' and multiplying the resulting equation with $\partial S_i/\partial w$ as

$$\frac{\partial\mathbf{H}}{\partial w'}\cdot\frac{\partial S_i}{\partial w}=\sum_{p=0}^{\infty}\int d\mathbf{P}\int dE''\int d\mathbf{\Omega}''\int d\mathbf{P}_{p-1}\cdots\int d\mathbf{P}_0\int d\mathbf{r}'\,U_{w'}^{\mathbf{H}}u_w^{Si}$$
$$\cdot\begin{Bmatrix}C_{\mathrm{f}}(\mathbf{r};E'',\mathbf{\Omega}''\to E,\mathbf{\Omega})K_s(\mathbf{P}_{p-1}\to\mathbf{r},E'',\mathbf{\Omega}'')\cdots\\ \cdot K_S(\mathbf{P}_0\to\mathbf{P}_1)T(E_0,\mathbf{\Omega}_0;\mathbf{r}'\to\mathbf{r}_0)\end{Bmatrix}S_i(\mathbf{r}',E_0,\mathbf{\Omega}_0) \tag{2.60}$$

The second-order sensitivity coefficient of S_i with respect to *x* and *y*, $u_{xy}^{S_i}$, to estimate $\mathbf{H}(\partial^2 S/\partial x\partial y)$ in Eq. (2.14) can be obtained by taking a second derivative for Eq. (2.15) with respect to *x*, *y* and dividing the resulting equation with the FSD, S_i, as

$$\begin{aligned}u_{xy}^{Si}&=\frac{1}{S_i}\frac{\partial^2 S_i}{\partial x\partial y}=\frac{1}{S_i}\frac{\partial}{\partial x}\left[\frac{\partial}{\partial y}\left(\frac{1}{k_{i-1}}\mathbf{H}S_{i-1}\right)\right]\\&=\frac{1}{S_i}\frac{\partial}{\partial x}\left[\frac{1}{k_{i-1}}\frac{\partial}{\partial y}(\mathbf{H}S_{i-1})-\frac{1}{k_{i-1}^2}\frac{\partial k_{i-1}}{\partial y}\mathbf{H}S_{i-1}\right]\\&=\frac{1}{k_{i-1}S_i}\frac{\partial^2}{\partial x\partial y}[\mathbf{H}S_{i-1}]-\frac{1}{k_{i-1}}\frac{\partial^2 k_{i-1}}{\partial x\partial y}-\frac{1}{k_{i-1}}\frac{\partial k_{i-1}}{\partial x}\left(\frac{1}{k_{i-1}S_i}\frac{\partial}{\partial y}[\mathbf{H}S_{i-1}]-\frac{1}{k_{i-1}}\frac{\partial k_{i-1}}{\partial y}\right)\\&\quad-\frac{1}{k_{i-1}}\frac{\partial k_{i-1}}{\partial y}\left(\frac{1}{k_{i-1}S_i}\frac{\partial}{\partial x}[\mathbf{H}S_{i-1}]-\frac{1}{k_{i-1}}\frac{\partial k_{i-1}}{\partial x}\right).\end{aligned} \tag{2.61}$$

By introducing Eqs. (2.2) and (2.3), the first term in RHS of Eq. (2.61) can

be written with explicit transport kernels as

$$\frac{1}{k_{i-1}\cdot S_i}\frac{\partial^2}{\partial x\partial y}\left[\mathbf{H}S_{i-1}\right]=\frac{1}{k_{i-1}\cdot S_i(\mathbf{P})}\left\{\begin{array}{l}\displaystyle\sum_{p=0}^{\infty}\int dE''\int d\mathbf{\Omega}''\int d\mathbf{P}_{p-1}\cdots\int d\mathbf{P}_0\int d\mathbf{r}'\,U_{xy}^{\mathbf{H}S}\\ \cdot C_{\mathrm{f}}\left(\mathbf{r};E'',\mathbf{\Omega}''\to E,\mathbf{\Omega}\right)K_s\left(\mathbf{P}_{p-1}\to\mathbf{r},E'',\mathbf{\Omega}''\right)\cdots\\ \cdot K_S\left(\mathbf{P}_0\to\mathbf{P}_1\right)T\left(E_0,\mathbf{\Omega}_0;\mathbf{r}'\to\mathbf{r}_0\right)S_{i-1}\left(\mathbf{r}',E_0,\mathbf{\Omega}_0\right)\end{array}\right\} \tag{2.62}$$

where,

$$U_{xy}^{\mathbf{H}S}=U_{xy}^{\mathbf{H}}+U_x^{\mathbf{H}}U_y^{\mathbf{H}}+U_x^{\mathbf{H}}u_y^{Si}+U_y^{\mathbf{H}}u_x^{Si}+u_{xy}^{Si}. \tag{2.63}$$

In the MC random work simulation, Eq. (2.60) can be estimated by

$$\left(\frac{1}{k_{i-1}\cdot S_i}\frac{\partial^2}{\partial x\partial y}\left[\mathbf{H}S_{i-1}\right]\right)_{j'p}=U_{xy,j'p}^{\mathbf{H}S} \tag{2.64}$$

where $U_{xy,j'p}^{\mathbf{H}S}$ denotes a value of $U_{xy}^{\mathbf{H}S}$ defined by Eq. (2.63) at the p-th collision site of j'-th history from which fission source neutrons generated for the next cycle. Using Eqs. (2.2), (2.3), and (2.16), the second term in RHS of Eq. (2.61) can be expressed as

$$\frac{\left\langle\frac{\partial^2}{\partial x\partial y}\left[\mathbf{HS}_{i-1}\right]\right\rangle}{\left\langle\mathbf{HS}_{i-1}\right\rangle}=\frac{\begin{array}{l}\displaystyle\sum_{p=0}^{\infty}\int d\mathbf{P}\int dE''\int d\mathbf{\Omega}''\int d\mathbf{P}_{p-1}\cdots\int d\mathbf{P}_0\int d\mathbf{r}'U_{xy}^{\mathbf{HS}}\\ \cdot\left\{\begin{array}{l}C_{\mathrm{f}}\left(\mathbf{r};E'',\mathbf{\Omega}''\to E,\mathbf{\Omega}\right)K_s\left(\mathbf{P}_{p-1}\to\mathbf{r},E'',\mathbf{\Omega}''\right)\cdots\\ \cdot K_S\left(\mathbf{P}_0\to\mathbf{P}_1\right)T\left(E_0,\mathbf{\Omega}_0;\mathbf{r}'\to\mathbf{r}_0\right)S_{i-1}\left(\mathbf{r}',E_0,\mathbf{\Omega}_0\right)\end{array}\right\}\end{array}}{\begin{array}{l}\displaystyle\sum_{p=0}^{\infty}\int d\mathbf{P}\int dE''\int d\mathbf{\Omega}''\int d\mathbf{P}_{p-1}\cdots\int d\mathbf{P}_0\int d\mathbf{r}'\\ \cdot\left\{\begin{array}{l}C_{\mathrm{f}}\left(\mathbf{r};E'',\mathbf{\Omega}''\to E,\mathbf{\Omega}\right)K_s\left(\mathbf{P}_{p-1}\to\mathbf{r},E'',\mathbf{\Omega}''\right)\cdots\\ \cdot K_S\left(\mathbf{P}_0\to\mathbf{P}_1\right)T\left(E_0,\mathbf{\Omega}_0;\mathbf{r}'\to\mathbf{r}_0\right)S_{i-1}\left(\mathbf{r}',E_0,\mathbf{\Omega}_0\right)\end{array}\right\}\end{array}}. \tag{2.65}$$

In the MC simulation, Eq. (2.65) can be estimated by

$$U^{k}_{xy,(i-1)} \equiv \left(\frac{1}{\langle \mathbf{HS}_{i-1} \rangle} \left\langle \frac{\partial^2}{\partial x \partial y} [\mathbf{HS}_{i-1}] \right\rangle \right)_{j'p} = \frac{\sum_{j'} \sum_{p} U^{\mathbf{HS}}_{xy,j'p} n_{f,(i-1)j'p}}{\sum_{j'} \sum_{p} n_{f,(i-1)j'p}}. \quad (2.66)$$

Then, $u^{S_{ij}}_{xy}$ can be estimated by

$$u^{S_{ij}}_{xy} = U^{\mathbf{HS}}_{xy,j'p} - U^{k}_{xy,(i-1)} - U^{k}_{x,(i-1)} u^{S_{(i-1)j'}}_{y} - U^{k}_{y,(i-1)} u^{S_{(i-1)j'}}_{x} \quad (2.67)$$

Assuming $u^{S_{i-n}}_{xy}$, $u^{S_{i-n}}_{x}$, and $u^{S_{i-n}}_{y}$ to be zero in the same way to calculate $u^{S_{ij}}_{w}$ in the first-order FSP method, the second-order sensitivity coefficient of S_i can be obtained recursively in the iteration process.

Then the reactivity coefficient sensitivity of a design parameter *y* to cross section *x*, $\partial^2 \rho / \partial x \partial y$, can be estimated by Eqs. (2.12), (2.13) and (2.14) using the k derivatives calculated by Eqs. (2.17), (2.37), (2.38), (2.60) and (2.67).

2.6. Sensitivity of the Temperature Coefficient

Suppose that the static reactivity ρ is a function of input parameters σ^{i}_{α} and T_r representing α-type reaction cross section of *i*-isotope and the system temperature of *r*-region. Then FTC can be estimated by taking a derivative of the reactivity with respect to fuel temperature. Eq. (2.68) describes the way to estimate fuel temperature coefficient.

$$\frac{d\rho\left(\cdots,\sigma_\alpha^i,\cdots,\mathrm{T}_r,\cdots\right)}{d\mathrm{T}_f}=\frac{1}{k^2}\frac{dk\left(\cdots,\sigma_\alpha^i,\cdots,\mathrm{T}_r,\cdots\right)}{d\mathrm{T}_f}$$
$$\cong\frac{1}{k^2}\left(\sum_i\sum_\alpha\frac{\partial k}{\partial\sigma_\alpha^i}\cdot\frac{d\sigma_\alpha^i}{d\mathrm{T}_f}+\frac{\partial k}{\partial\mathrm{T}_f}\cdot\frac{d\mathrm{T}_f}{d\mathrm{T}_f}\right) \tag{2.68}$$
$$\cong\frac{1}{k^2}\left(\sum_i\sum_\alpha\frac{\partial k}{\partial\sigma_\alpha^i}\cdot\frac{\Delta\sigma_\alpha^i}{\Delta\mathrm{T}_f}+\frac{\partial k}{\partial\mathrm{T}_f}\right)$$

The sensitivity of FTC can be estimated by taking a derivative of Eq. (2.10) with respect to fuel temperature. The sensitivity of FTC with respect to cross section, x is expressed in Eq. (2.69)

$$\frac{\partial}{\partial x}\left(\frac{d\rho}{d\mathrm{T}_f}\right)\cong\frac{\partial}{\partial x}\left[\frac{1}{k^2}\left(\sum_i\sum_\alpha\frac{\partial k}{\partial\sigma_\alpha^i}\cdot\frac{\Delta\sigma_\alpha^i}{\Delta\mathrm{T}_f}+\frac{\partial k}{\partial\mathrm{T}_f}\right)\right]$$
$$\cong-\frac{2}{k^3}\frac{\partial k}{\partial x}\cdot\left(\sum_i\sum_\alpha\frac{\partial k}{\partial\sigma_\alpha^i}\cdot\frac{\Delta\sigma_\alpha^i}{\Delta\mathrm{T}_f}+\frac{\partial k}{\partial\mathrm{T}_f}\right)$$
$$+\frac{1}{k^2}\cdot\frac{\partial}{\partial x}\left(\sum_i\sum_\alpha\frac{\partial k}{\partial\sigma_\alpha^i}\cdot\frac{\Delta\sigma_\alpha^i}{\Delta\mathrm{T}_f}+\frac{\partial k}{\partial\mathrm{T}_f}\right) \tag{2.69}$$
$$\cong-\frac{2}{k^3}\frac{\partial k}{\partial x}\cdot\left(\sum_i\sum_\alpha\frac{\partial k}{\partial\sigma_\alpha^i}\cdot\frac{\Delta\sigma_\alpha^i}{\Delta\mathrm{T}_f}+\frac{\partial k}{\partial\mathrm{T}_f}\right)$$
$$+\frac{1}{k^2}\left(\sum_i\sum_\alpha\frac{\partial^2 k}{\partial x\partial\sigma_\alpha^i}\cdot\frac{\Delta\sigma_\alpha^i}{\Delta\mathrm{T}_f}\right)+\frac{1}{k^2}\frac{\partial}{\partial x}\left(\frac{\partial k}{\partial\mathrm{T}_f}\right)$$

The fuel temperature change is converted into the corresponding variations in both the microscopic cross sections and the Doppler broadened scattering collision kernel [10]. There are two terms of the second-order derivatives of k in Eq. (2.69). The first term has the variable of x as cross section for the sensitivity and y for cross section as a response variable by the fuel temperature change. In this case, the first-order and second-order sensitivity

coefficient of kernels can be easily obtained and $\Delta\sigma_\alpha^i$ is calculated by subtraction of two different cross sections in the different temperature. The second term has variables of *x*, fuel temperature T_f. The first-order and second-order sensitivity coefficients of Doppler broadened scattering kernels are described as follows. The first-order *k* sensitivity to fuel temperature can be written with the explicit transport kernels as

$$\begin{aligned}\frac{\partial k}{\partial \mathrm{T}_f} = \sum_{p=0}^{\infty}\int d\mathbf{P}\int dE''\int d\mathbf{\Omega}''\int d\mathbf{P}_{p-1}\cdots\int d\mathbf{P}_0\int d\mathbf{r}'\left(U_{\mathrm{T}_f}^{\mathbf{H}}+u_{\mathrm{T}_f}^{S_i}\right)\\ \cdot\begin{Bmatrix} C_f\left(\mathbf{r};E'',\mathbf{\Omega}''\to E,\mathbf{\Omega}\right)T\left(\mathbf{r}_{p-1},E'',\mathbf{\Omega}''\to\mathbf{r},E'',\mathbf{\Omega}''\right)\\ \cdots C_S\left(\mathbf{r}_0,E_0,\mathbf{\Omega}_0\to E_1,\mathbf{\Omega}_1\right)T\left(E_0,\mathbf{\Omega}_0;\mathbf{r}'\to\mathbf{r}_0\right)\end{Bmatrix}\\ \cdot S_i\left(\mathbf{r}',E_0,\mathbf{\Omega}_0\right).\end{aligned} \tag{2.70}$$

$U_{\mathrm{T}_f}^{\mathbf{H}}$ can be expressed with the sensitivity coefficients of the collision kernel with respect to fuel temperature T_f as

$$U_{\mathrm{T}_f}^{\mathbf{H}} \equiv u_{\mathrm{T}_f}^{C}(\mathbf{P}_{p-1}\to\mathbf{r}_{p-1},E'',\mathbf{\Omega}'')+\sum_{p'=0}^{p-2}u_{\mathrm{T}_f}^{C}(\mathbf{P}_{p'}\to\mathbf{r}_{p'},E_{p'+1},\mathbf{\Omega}_{p'+1}); \tag{2.71}$$

and the first-order sensitivity coefficient of the collision kernel $u_{\mathrm{T}_f}^{C_s}$ is

$$u_{\mathrm{T}_f}^{C}(\mathbf{P}_{p'}\to\mathbf{r}_{p'},E_{p'+1},\mathbf{\Omega}_{p'+1})=\frac{1}{C_s(\mathbf{P}_{p'}\to\mathbf{r}_{p'},E_{p'+1},\mathbf{\Omega}_{p'+1})}\frac{C_s(\mathbf{P}_{p'}\to\mathbf{r}_{p'},E_{p'+1},\mathbf{\Omega}_{p'+1})}{\partial\mathrm{T}_f}. \tag{2.72}$$

In MC random walk process, when a neutron makes a reaction of type "a" with isotope *j*' at energy *E*' and **Ω**' is scattered to *E* and **Ω**, the sampled scattering collision kernel can be written as

$$C_s\left(\mathbf{r}';E',\mathbf{\Omega}'\to E,\mathbf{\Omega}\right)=\nu_a^{j'}\frac{N^{j'}\sigma_a^{j'}(E')}{\Sigma_t(E')}f_a^{j'}(E',\mathbf{\Omega}'\to E,\mathbf{\Omega}). \tag{2.73}$$

Further, one can consider the target velocity with free-monatomic-gas model and the collision kernel can be modified as

$$C_s\left(\mathbf{r}';E',\mathbf{\Omega}'\to E,\mathbf{\Omega}\right)=\nu_a^{j'}\frac{N^{j'}\sigma_a^{j'}(E')}{\Sigma_t(E')}P^{j'}\left(V,\mu_t\middle|\mathrm{T}_r\right)f_a^{j'}(E'_{rel},\mathbf{\Omega}'_{rel}\to E,\mathbf{\Omega}),$$

(2.74)

$P^{j'}\left(V,\mu_t\middle|\mathrm{T}_r\right)$ is the probability function about the target *j*'s speed V and direction μ_t on the region temperature T_r. E'_{rel} and $\mathbf{\Omega}'_{\mathrm{rel}}$ indicate the relative neutron energy and direction with considering the target velocity. $u_{\mathrm{T}_f}^C$ in Eq. (2.72) can be expressed by

$$\begin{aligned}u_{\mathrm{T}}^C&=\frac{1}{C_s\left(\mathbf{r}';E',\mathbf{\Omega}'\to E,\mathbf{\Omega}\right)}\frac{\partial C_s\left(\mathbf{r}';E',\mathbf{\Omega}'\to E,\mathbf{\Omega}\right)}{\partial\mathrm{T}_f}\\&=\left(\nu_a^{j'}\frac{N^{j'}\sigma_a^{j'}(E')}{\Sigma_t(E')}P^{j'}\left(V,\mu_t\middle|\mathrm{T}_r\right)f_a^{j'}(E'_{rel},\mathbf{\Omega}'_{rel}\to E,\mathbf{\Omega})\right)^{-1}\\&\cdot\frac{\partial}{\partial\mathrm{T}_f}\left(\nu_a^{j'}\frac{N^{j'}\sigma_a^{j'}(E')}{\Sigma_t(E')}P^{j'}\left(V,\mu_t\middle|\mathrm{T}_r\right)f_a^{j'}(E'_{rel},\mathbf{\Omega}'_{rel}\to E,\mathbf{\Omega})\right)\\&=\frac{1}{P^{j'}\left(V,\mu_t\middle|\mathrm{T}\right)}\frac{\partial P^{j'}\left(V,\mu_t\middle|\mathrm{T}_f\right)}{\partial\mathrm{T}_f}.\end{aligned}\tag{2.75}$$

When we use Free-monatomic-gas model with constant cross section, the $P^{j'}$ can be written as

$$P^{j'}=P_{CXS}^{j'}\left(V,\mu\middle|\mathrm{T}_r\right)=\frac{v_{rel}p\left(\beta_{j'},V\right)}{2g\left(\alpha_{j'}\right)v_n}\tag{2.76}$$

where,

$$p\left(\beta_{j'},V\right)=\frac{4}{\sqrt{\pi}}\beta_{j'}^{3}V^{2}e^{-\beta_{j'}^{2}V^{2}};\quad \beta_{j'}=\sqrt{\frac{A_{j'}M_{n}}{2k_{B}\mathrm{T}_{r}}},$$
$$g\left(\alpha_{j'}\right)\equiv\frac{1}{\alpha_{j'}^{2}}\left[\left(\alpha_{j'}^{2}+\frac{1}{2}\right)\mathrm{erf}\left(\alpha_{j'}\right)+\frac{1}{\sqrt{\pi}}\alpha_{j'}\exp\left(-\alpha_{j'}^{2}\right)\right];\quad \alpha_{j'}\equiv\beta_{j'}v_{n} \tag{2.77}$$

$v_n =$ neutron speed
$M_n =$ rest mass of neutron
$A_{j'} =$ atomic mass ratio of nu

The first-order sensitivity coefficient of the scattering collision kernel with respect to temperature can be written as

$$\begin{aligned}
u_{\mathrm{T}_f}^{C} &= \frac{1}{P_{CXS}^{j'}\left(V,\mu\middle|\mathrm{T}_r\right)}\frac{\partial P_{CXS}^{j'}\left(V,\mu\middle|\mathrm{T}_r\right)}{\partial \mathrm{T}_f} \\
&= \frac{2v_n g\left(\alpha_{j'}\right)}{v_{rel}p\left(\beta_{j'},V\right)}\cdot\frac{\partial}{\partial \mathrm{T}_f}\left(\frac{v_{rel}}{2v_n}\frac{p\left(\beta_{j'},V\right)}{g\left(\alpha_{j'}\right)}\right) \\
&= \frac{g\left(\alpha_{j'}\right)}{p\left(\beta_{j'},V\right)}\cdot\left(-\frac{p\left(\beta_{j'},V\right)}{g\left(\alpha_{j'}\right)^{2}}\cdot\frac{\partial g\left(\alpha_{j'}\right)}{\partial \mathrm{T}_f}+\frac{1}{g\left(\alpha_{j'}\right)}\cdot\frac{\partial p\left(\beta_{j'},V\right)}{\partial \mathrm{T}_f}\right) \\
&= -\frac{1}{g\left(\alpha_{j'}\right)}\cdot\frac{\partial g\left(\alpha_{j'}\right)}{\partial \mathrm{T}_f}+\frac{1}{p\left(\beta_{j'},V\right)}\cdot\frac{\partial p\left(\beta_{j'},V\right)}{\partial \mathrm{T}_f}
\end{aligned} \tag{2.78}$$

The first term in Eq. (2.78) can be written as

$$
\begin{aligned}
-\frac{1}{g\left(\beta_{j'}v_n\right)}\cdot\frac{\partial g\left(\beta_{j'}v_n\right)}{\partial \mathrm{T}_f} &= -\frac{1}{g\left(\alpha_{j'}\right)}\cdot\frac{\partial}{\partial \mathrm{T}_f}\left\{\frac{1}{\alpha_{j'}^2}\left[\begin{array}{l}\left(\alpha_{j'}^2+\frac{1}{2}\right)\mathrm{erf}\left(\alpha_{j'}\right)\\ +\frac{\alpha_{j'}}{\sqrt{\pi}}\exp\left(-\alpha_{j'}^2\right)\end{array}\right]\right\}\\
&= -\frac{1}{g\left(\alpha_{j'}\right)}\frac{\partial}{\partial \mathrm{T}_f}\left(\frac{1}{\alpha_{j'}^2}\right)\left[\begin{array}{l}\left(\alpha_{j'}^2+\frac{1}{2}\right)\mathrm{erf}\left(\alpha_{j'}\right)\\ +\frac{\alpha_{j'}}{\sqrt{\pi}}\exp\left(-\alpha_{j'}^2\right)\end{array}\right]\\
&\quad -\frac{1}{g\left(\alpha_{j'}\right)}\frac{1}{\alpha_{j'}^2}\frac{\partial}{\partial \mathrm{T}_f}\left[\begin{array}{l}\left(\alpha_{j'}^2+\frac{1}{2}\right)\mathrm{erf}\left(\alpha_{j'}\right)\\ +\frac{\alpha_{j'}}{\sqrt{\pi}}\exp\left(-\alpha_{j'}^2\right)\end{array}\right]\\
&= -\alpha_{j'}^2\cdot\left(-\frac{2\alpha_{j'}}{\alpha_{j'}^4}\frac{\partial\alpha_{j'}}{\partial \mathrm{T}_f}\right)\\
&\quad -\frac{1}{g\left(\alpha_{j'}\right)}\frac{1}{\alpha_{j'}^2}\frac{\partial}{\partial \mathrm{T}_f}\left[\left(\alpha_{j'}^2+\frac{1}{2}\right)\mathrm{erf}\left(\alpha_{j'}\right)+\frac{\alpha_{j'}}{\sqrt{\pi}}\exp\left(-\alpha_{j'}^2\right)\right]\\
&= \frac{1}{\alpha_{j'}}\frac{\partial\alpha_{j'}}{\partial \mathrm{T}_f}-\frac{1}{\alpha_{j'}^2}\frac{1}{g\left(\alpha_{j'}\right)}\\
&\quad \cdot\left[\begin{array}{l}\left(2\alpha_{j'}\frac{\partial\alpha_{j'}}{\partial \mathrm{T}_f}\right)\mathrm{erf}\left(\alpha_{j'}\right)+\left(\alpha_{j'}^2+\frac{1}{2}\right)\frac{\partial\mathrm{erf}\left(\alpha_{j'}\right)}{\partial \mathrm{T}_f}\\ +\frac{1}{\sqrt{\pi}}\frac{\partial\alpha_{j'}}{\partial \mathrm{T}_f}\exp\left(-\alpha_{j'}^2\right)+\frac{\alpha_{j'}}{\sqrt{\pi}}\exp\left(-\alpha_{j'}^2\right)\left(-2\alpha_{j'}\right)\frac{\partial\alpha_{j'}}{\partial \mathrm{T}_f}\end{array}\right],
\end{aligned}
\tag{2.79}
$$

Eq. (2.79) can be modified as

$$
\begin{aligned}
-\frac{1}{g\left(\beta_{j'}v_n\right)}\cdot\frac{\partial g\left(\beta_{j'}v_n\right)}{\partial \mathrm{T}_f} &= \frac{1}{\alpha_{j'}}\frac{\partial \alpha_{j'}}{\partial \mathrm{T}_f}-\frac{1}{\alpha_{j'}^2}\frac{1}{g\left(\alpha_{j'}\right)} \\
&\cdot\left[\begin{array}{l}\left(2\alpha_{j'}\dfrac{\partial \alpha_{j'}}{\partial \mathrm{T}_f}\right)\mathrm{erf}\left(\alpha_{j'}\right)+\left(\alpha_{j'}^2+\dfrac{1}{2}\right)\dfrac{\partial \mathrm{erf}\left(\alpha_{j'}\right)}{\partial \mathrm{T}_f} \\ +\left(1-2\alpha_{j'}^2\right)\dfrac{1}{\sqrt{\pi}}\dfrac{\partial \alpha_{j'}}{\partial \mathrm{T}_f}\exp\left(-\alpha_{j'}^2\right)\end{array}\right] \\
&= \frac{1}{\alpha_{j'}}\frac{\partial \alpha_{j'}}{\partial \mathrm{T}_f}-\frac{1}{\alpha_{j'}^2}\frac{1}{g\left(\alpha_{j'}\right)} \\
&\cdot\left[\begin{array}{l}\left(2\alpha_{j'}\dfrac{\partial \alpha_{j'}}{\partial \mathrm{T}_f}\right)\mathrm{erf}\left(\alpha_{j'}\right)+\left(\alpha_{j'}^2+\dfrac{1}{2}\right)\dfrac{\partial \mathrm{erf}\left(\alpha_{j'}\right)}{\partial \mathrm{T}_f} \\ +\left(\dfrac{1}{2}-\alpha_{j'}^2\right)\dfrac{\partial \mathrm{erf}\left(\alpha_{j'}\right)}{\partial \mathrm{T}_f}\end{array}\right] \\
&= \frac{1}{\alpha_{j'}}\frac{\partial \alpha_{j'}}{\partial \mathrm{T}_f}-\frac{1}{g\left(\alpha_{j'}\right)}\left[\left(\frac{2}{\alpha_{j'}}\frac{\partial \alpha_{j'}}{\partial \mathrm{T}_f}\right)\mathrm{erf}\left(\alpha_{j'}\right)+\frac{1}{\alpha_{j'}^2}\frac{\partial \mathrm{erf}\left(\alpha_{j'}\right)}{\partial \mathrm{T}_f}\right].
\end{aligned}
\tag{2.80}
$$

The second term in Eq. (2.78) can be written as

$$
\begin{aligned}
\frac{1}{p\left(\beta_{j'},V\right)}\frac{\partial p\left(\beta_{j'},V\right)}{\partial \mathrm{T}_f} &= \frac{1}{p\left(\beta_{j'},V\right)}\frac{\partial p\left(\beta_{j'},V\right)}{\partial \beta_{j'}} \\
&= \frac{1}{\frac{4}{\sqrt{\pi}}\beta_{j'}^3 V^2 \exp\left(-\beta_{j'}^2 V^2\right)} \\
&\quad \cdot \left(\begin{array}{l} \frac{4}{\sqrt{\pi}} 3\beta_{j'}^2 V^2 \exp\left(-\beta_{j'}^2 V^2\right) \\ +\left(-2\beta_{j'} V^2\right)\frac{4}{\sqrt{\pi}}\beta_{j'}^3 V^2 \exp\left(-\beta_{j'}^2 V^2\right) \end{array} \right) \cdot \frac{\partial \beta_{j'}}{\partial \mathrm{T}_f} \\
&= \frac{1}{\beta_{j'} \cancel{\frac{4}{\sqrt{\pi}}\beta_{j'}^2 V^2 \exp\left(-\beta_{j'}^2 V^2\right)}} \\
&\quad \cdot \left[3-2\beta_{j'}^2 V^2\right] \cancel{\frac{4}{\sqrt{\pi}}\beta_{j'}^2 V^2 \exp\left(-\beta_{j'}^2 V^2\right)} \frac{\partial \beta_{j'}}{\partial \mathrm{T}_f} \\
&= \frac{3-2\beta_{j'}^2 V^2}{\beta_{j'}} \cdot \frac{\partial \beta_{j'}}{\partial \mathrm{T}_f} \\
&= \left[3-2\alpha_{j'}^2\left(\frac{V}{v_n}\right)^2\right] \cdot \frac{1}{\beta_{j'}}\frac{\partial \beta_{j'}}{\partial \mathrm{T}_f}
\end{aligned}
\tag{2.81}
$$

$1/\alpha_{j'} \cdot \partial \alpha_{j'}/\partial \mathrm{T}_f$ and $1/\beta_{j'} \cdot \partial \beta_{j'}/\partial \mathrm{T}_f$ in Eq. (2.78) and Eq. (2.79) can be written as

$$
\begin{aligned}
\frac{1}{\alpha_{j'}}\frac{\partial \alpha_{j'}}{\partial \mathrm{T}_f} &= \frac{1}{\beta_{j'}}\frac{\partial \beta_{j'}}{\partial \mathrm{T}_f} \\
&= \sqrt{\frac{A_{j'} M_n}{2k_B \mathrm{T}_f}}^{-1} \cdot \frac{1}{2}\sqrt{\frac{A_{j'} M_n}{2k_B \mathrm{T}_f}}^{-1} \cdot \left(-\frac{A_{j'} M_n}{2k_B \mathrm{T}_f}\frac{1}{\mathrm{T}_f}\right) \\
&= -\frac{1}{2\mathrm{T}_f}.
\end{aligned}
\tag{2.82}
$$

Then, by insertions of Eq. (2.82) into Eq. (2.80) and Eq. (2.81), the resulting equations are expressed as

$$-\frac{1}{g\left(\beta_{j'},v_n\right)}\cdot\frac{\partial g\left(\beta_{j'},v_n\right)}{\partial \mathrm{T}_f}=\frac{1}{\alpha_{j'}}\frac{\partial\alpha_{j'}}{\partial \mathrm{T}_f}-\frac{1}{g\left(\alpha_{j'}\right)}\left[\begin{array}{l}\dfrac{2}{\alpha_{j'}}\dfrac{\partial\alpha_{j'}}{\partial \mathrm{T}_f}\mathrm{erf}\left(\alpha_{j'}\right)\\ +\dfrac{1}{2\alpha_{j'}}\dfrac{\partial\mathrm{erf}\left(\alpha_{j'}\right)}{\partial\alpha_{j'}}\cdot\dfrac{2}{\alpha_{j'}}\dfrac{\partial\alpha_{j'}}{\partial \mathrm{T}_f}\end{array}\right]$$

$$=\left\{-0.5+\frac{1}{g\left(\alpha_{j'}\right)}\left[\mathrm{erf}\left(\alpha_{j'}\right)+\frac{1}{2\alpha_{j'}}\frac{\partial\mathrm{erf}\left(\alpha_{j'}\right)}{\partial\alpha_{j'}}\right]\right\}\frac{1}{\mathrm{T}_f} \tag{2.83}$$

$$\frac{1}{p\left(\beta_{j'},V\right)}\frac{\partial p\left(\beta_{j'},V\right)}{\partial \mathrm{T}_f}=\left[-1.5+\alpha_{j'}^2\left(\frac{V}{v_n}\right)^2\right]\cdot\frac{1}{\mathrm{T}_f} \tag{2.84}$$

Thus, the sensitivity coefficient of the collision kernel can be calculated by

$$\begin{aligned}u_{\mathrm{T}_f}^{C_s}&=-\frac{1}{g\left(\beta_{j'},v_n\right)}\cdot\frac{\partial g\left(\beta_{j'},v_n\right)}{\partial \mathrm{T}_f}+\frac{1}{p\left(\beta_{j'},V\right)}\cdot\frac{\partial p\left(\beta_{j'},V\right)}{\partial \mathrm{T}_f}\\&=\left\{\begin{array}{l}-2.5+\alpha_{j'}^2\left(\dfrac{V}{v_n}\right)^2\\ +\dfrac{1}{g\left(\alpha_{j'}\right)}\left[\mathrm{erf}\left(\alpha_{j'}\right)+\dfrac{1}{2\alpha_{j'}}\dfrac{\partial\left[\mathrm{erf}\left(\alpha_{j'}\right)\right]}{\partial \mathrm{T}_f}\right]\end{array}\right\}\cdot\left(\frac{1}{\mathrm{T}_f}\right).\end{aligned} \tag{2.85}$$

Then, the sensitivity coefficient of S_i can be estimated by using Eq. (2.38)

$$u_{\mathrm{T}_f}^{S_{ij}}=U_{\mathrm{T}_f,(i-1)j'p}^{\mathbf{H}S}-U_{\mathrm{T}_f,(i-1)}^{k} \tag{2.86}$$

$U_{\mathrm{T}_f,(i-1)j'p}^{\mathbf{H}S}$ denotes the value of $U_{\mathrm{T}_f,(i-1)}^{\mathbf{H}}$ of Eq. (2.71) plus $u_{T_f}^{S_{(i-1)}}$ at the p-th collision site of j'-th history where neutron generated in (i-1) cycle. $u_{\mathrm{T}_f}^{S(i-1)j'}$ denotes the first-order sensitivity coefficient of $S_{i\text{-}1}$ as described in Eq. (2.37) for the j'-th history in cycle i-1.

The second-order derivative of k with respect to cross section and fuel temperature in Eq. (2.69) can be written with transport kernels as

$$\begin{aligned}\frac{\partial^2 k}{\partial x \partial \mathrm{T}_f} = & \sum_{p=0}^{\infty} \int d\mathbf{P} \int dE'' \int d\mathbf{\Omega}'' \int d\mathbf{P}_{p-1} \cdots \int d\mathbf{P}_0 \int d\mathbf{r}' \, U_{x\mathrm{T}_f}^{\mathbf{H}S} \\ & \cdot \left\{ \begin{array}{l} C_{\mathrm{f}}\left(\mathbf{r}; E'', \mathbf{\Omega}'' \to E, \mathbf{\Omega}\right) T\left(\mathbf{r}_{p-1}, E'', \mathbf{\Omega}'' \to \mathbf{r}, E'', \mathbf{\Omega}''\right) \\ \cdots C_s\left(\mathbf{r}_0, E_0, \mathbf{\Omega}_0 \to E_1, \mathbf{\Omega}_1\right) T\left(E_0, \mathbf{\Omega}_0; \mathbf{r}' \to \mathbf{r}_0\right) \end{array} \right\} \\ & \cdot S_i\left(\mathbf{r}', E_0, \mathbf{\Omega}_0\right).\end{aligned} \tag{2.87}$$

where

$$U_{x\mathrm{T}_f}^{\mathbf{H}S} = U_{x\mathrm{T}_f}^{\mathbf{H}} + U_x^{\mathbf{H}} U_{\mathrm{T}_f}^{\mathbf{H}} + U_x^{\mathbf{H}} u_{\mathrm{T}_f}^{Si} + U_{\mathrm{T}_f}^{\mathbf{H}} u_x^{Si} + u_{x\mathrm{T}_f}^{Si}. \tag{2.88}$$

$U_{x\mathrm{T}_f}^{\mathbf{H}}$ can be expressed with the second-order sensitivity coefficients of the collision kernels with respect to the temperature T_f and x as follows

$$U_{x\mathrm{T}_f}^{\mathbf{H}} \equiv u_{x\mathrm{T}_f}^{C_s}(\mathbf{P}_{p-1} \to \mathbf{r}_{p-1}, E'', \mathbf{\Omega}'') + \sum_{p'=0}^{p-2} u_{x\mathrm{T}_f}^{C_s}(\mathbf{P}_{p'} \to \mathbf{r}_{p'}, E_{p'+1}, \mathbf{\Omega}_{p'+1}). \tag{2.89}$$

The second-order sensitivity coefficient of the collision kernel $u_{x\mathrm{T}_f}^{C_s}$ is

$$\begin{aligned} u_{x\mathrm{T}_f}^{C_s} &= \frac{\partial}{\partial x}\left(u_{\mathrm{T}_f}^{C_s}\right) \\ &= \frac{\partial}{\partial x}\left\{-\frac{1}{g\left(\alpha_{j'}\right)} \cdot \frac{\partial g\left(\alpha_{j'}\right)}{\partial \mathrm{T}_f} + \frac{1}{p\left(\beta_{j'}, V\right)} \cdot \frac{\partial p\left(\beta_{j'}, V\right)}{\partial \mathrm{T}_f}\right\} \\ &= 0. \end{aligned} \tag{2.90}$$

The second-order sensitivity coefficient of S_i can be estimated by

$$u_{x\mathrm{T}_f}^{S_{ij}} = U_{x\mathrm{T}_f, j'k}^{\mathbf{H}S} - U_{x\mathrm{T}_f,(i-1)}^{k} - U_{x,(i-1)}^{k} u_{\mathrm{T}_f}^{S_{(i-1)j'}} - U_{\mathrm{T}_f,(i-1)}^{k} u_x^{S_{(i-1)j'}} \tag{2.91}$$

$U_{x\mathrm{T}_f, j'p}^{\mathbf{H}S}$ denotes the value of $U_{x\mathrm{T}_f}^{\mathbf{H}S}$ in Eq. (2.88) at the p-th collision site of j'-th history where neutron generated in cycle i-1.

Chapter 3. Effectiveness of the MC2P Method

3.1. Two-Group Infinite Homogeneous Problem of CANDU 6 Bundle model

The proposed MC2P algorithms based on Eq. (12) have been implemented in McCARD [16] and tested for a homogeneous two-group infinite problem for the CANDU 6 lattice model. The two-group cross sections for CANDU 6 lattice model are generated by McCARD. In following subsection 3.1.1, the B1 MC method to generate the diffusion group constants is briefly described. CANDU 6 lattice model description is introduced in subsection 3.1.2. The test results are suggested in subsection 3.1.3 and the results are suggested term by term in Eq. (2.12) to Eq. (2.14). Firstly, the first-order k sensitivities to x or y (x, y indicate the cross section and density or fuel temperature) are presented with the comparison results with the analytic solutions. Secondly, the second-order k derivatives are presented with the comparison results with the analytic solutions. Finally, the sensitivities of reactivity coefficient are presented with the comparison results with the analytic solutions.

3.1.1. Two-group diffusion constant generation

A detailed description of the B_1 MC method is available in [16, 17, 18]. In order to make this paper self-contained, it is briefly described here. The

essential step of the B_1 MC method involves infinite medium spectrum (IMS) calculations for angular flux $\phi(\mathbf{r},E,\mathbf{\Omega})$ by the MC neutron transport calculations, which are performed to determine fine-group cross sections of a nuclear fuel system like a fuel assemble or a fuel bundle defined as

$$\Sigma_{x,g}=\frac{\int_{\mathrm{V}}\int_{\Delta E_g}\int_{4\pi}\Sigma_x(\mathbf{r},E)\phi(\mathbf{r},E,\mathbf{\Omega})\,d\mathbf{\Omega}dEd\mathbf{r}}{\int_{\mathrm{V}}\int_{\Delta E_g}\int_{4\pi}\phi(\mathbf{r},E,\mathbf{\Omega})\,d\mathbf{\Omega}dEd\mathbf{r}}, \tag{3.1}$$

$$\Sigma^n_{s,g'g}=\frac{\int_{\mathrm{V}}\int_{\Delta E_g}\int_{\Delta E_{g'}}\int_{4\pi}\Sigma^n_s(\mathbf{r},E\to E')\phi(\mathbf{r},E,\mathbf{\Omega})\,d\mathbf{\Omega}dE'dEd\mathbf{r}}{\int_{\mathrm{V}}\int_{\Delta E_g}\int_{4\pi}\phi(\mathbf{r},E,\mathbf{\Omega})\,d\mathbf{\Omega}dEd\mathbf{r}}. \tag{3.2}$$

$\Sigma_{x,g}$ (x = scattering, absorption, fission) is the x-type IMS-weighted g-grourp reaction cross section of the nuclear system. $\Sigma^n_{s,g'g}$ (n = 0, 1) is the IMS-weighted n-th coefficient of Legendre expansion of group transfer scattering cross section. It must be noted that Eq. (3.2) for $\Sigma^1_{s,g'g}$ derives from an approximation that the energy dependence of the P_1 component of Legendre expansion of $\phi(\mathbf{r},E,\mathbf{\Omega})$ is proportional to P_0 component [16, 17, 18]. Once the IMS-weighted fine-group cross sections in Eq. (1) and (2) are obtained through the MC calculations, they are used to specify B_1 Equations:

$$\Sigma_{t,g}\phi_g \pm iBJ_g=\sum_{g'}\Sigma^0_{s,gg'}\phi_{g'}+\chi_{g'} \tag{3.3}$$

$$\pm iB\phi_g+3\alpha_g(B)\Sigma_{t,g}J_g=3\sum_{g'}\Sigma^1_{s,gg'}J_{g'}. \tag{3.4}$$

Like its deterministic counterparts, the B_1 MC method makes use of the solution to the B_1 equations above, namely, the critical spectrum (CS) ϕ_g^B, the critical current spectrum J_g^B, and the critical buckling B_c^2, to determine the CS-weighted few-group cross sections $\Sigma_{x,G}$ by

$$\Sigma_{x,G} = \frac{\sum_{g \in G} \Sigma_{x,g} \phi_g}{\sum_{g \in G} \phi_g} \tag{3.5}$$

and the few-group diffusion constants D_G by

$$D_G = \frac{\pm \sum_{g \in G} i J_g^B}{\sum_{g \in G} B_c \phi_g^B}. \tag{3.6}$$

The B_1 MC method has been implemented into the few-group generation module of the SNU MC code McCARD. The qualification of the method as a two-group constant generator for the standard unit lattice cell is examined in terms of the CANDU 6 core analysis problems described in [18].

3.1.2. Standard CANDU 6 bundle problem

Figure 3.1 shows the standard CANDU 6 bundle which comprises a 37-element fuel bundle, pressurized heavy-water coolant in a pressure tube, and the associated unpressurized heavy water moderator. Fuel material is the natural UO^2 and fuel density is 10.4919g/cm^3. Pressure tube thickness is 4.343mm and diameter is 103.378mm while Calandriatube thickness is 1.397mm and diameter is 128.956mm. Moderator material is a heavy water.

The fuel temperature is 960.2K and cladding temperature is 561.2K. The coolant temperature is 561.2K and moderator temperature is 342.2K. The two-group diffusion cross-sections are generated by McCARD for the CANDU 6 lattice cell problem. Fast group's lower energy boundary is 0.625 eV and all McCARD cross-section generation calculation are performed for 100 active cycles on 1,000,000 number of histories per cycle.

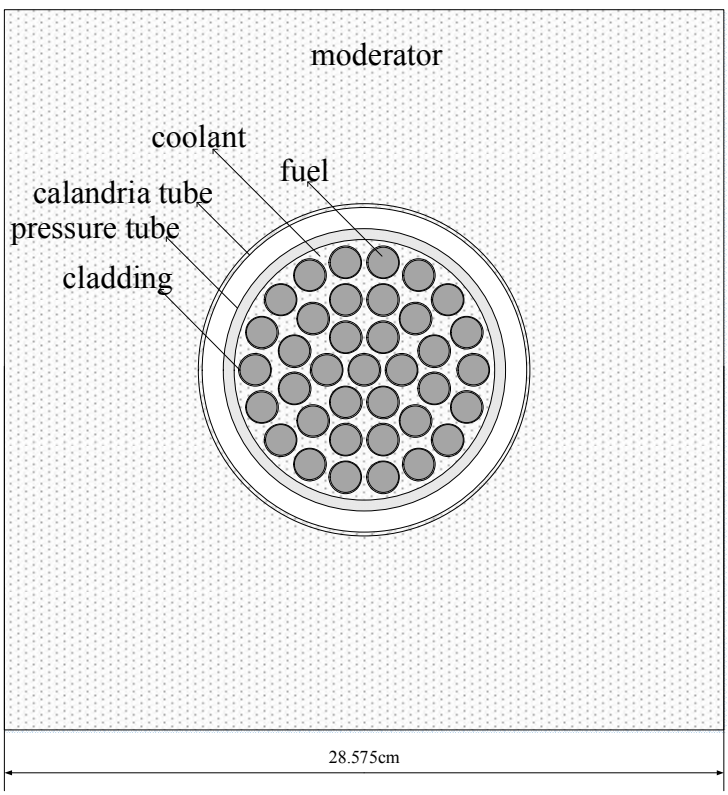

Figure 3.1 Standard CANDU 6 Bundle problem

3.1.3. Reactivity coefficient of moderator number density

The macroscopic cross section and microscopic cross section are generated for the fuel and coolant region (inside calandria tube region) and moderator

region for CANDU 6 bundle model [18]. Table 3.1 and 3.2 show two-group macroscopic cross sections for fuel-coolant-mixed medium and microscopic ones for moderator. Note that energy spectrum of fission neutron produced from a thermal fission reaction is modified to magnify the PSE for the verification purpose. The ν_1, ν_2 values and the moderator number density are set to 2.6649, 2.4367, and 9.792×10^{-2} per 10^{-24} cm^3, respectively. $\Sigma_{sg'g}$, and $\chi_{g'g}$ are the scattering cross section and energy spectrums of fission neutrons from energy group g to g'. Others follows standard. It is note that chi spectrum is modified. The McCARD eigenvalue calculation is performed on 40,000 active cycles with 200,000 number of histories per cycle. The propagation batch size is set to 5 for the PSE calculations.

Table 3.1. Two-group macroscopic cross sections for the fuel-coolant mixture of the infinite homogeneous problem

Cross section	Fuel-moderator mixture	
	Fast Gr.	Thermal Gr.
Σ_{tg}	3.953×10^{-2}	5.746×10^{-2}
Σ_{ag}	1.663×10^{-3}	3.439×10^{-3}
Σ_{fg}	3.310×10^{-4}	1.766×10^{-3}
Σ_{s1g}	3.089×10^{-2}	6.585×10^{-5}
Σ_{s2g}	0.000	5.401×10^{-2}
χ_{1g}	1.000	0.500
χ_{2g}	0.000	0.500

Table 3.2 Two-group microscopic cross sections for the moderator of the infinite homogeneous problem

Cross section	Moderator	
	Fast Gr.	Thermal Gr.
σ_{tg}	2.860×10^{0}	3.890×10^{0}
σ_{ag}	2.337×10^{-4}	4.941×10^{-4}
σ_{s1g}	2.770×10^{0}	4.105×10^{-4}
σ_{s2g}	8.984×10^{-2}	3.889×10^{0}

Table 3.3 shows the comparisons of k sensitivities to the moderator number density calculated by MC2P method with analytic solutions. N^{mod} indicates the density of moderator. Analytic solutions for k sensitivities and their POE and PSE terms are in the second column. The first-order POE and PSE indicate $\left\langle (\partial \mathbf{H}/\partial \mathrm{N}_{\mathrm{mod}})S \right\rangle$ and $\left\langle \mathbf{H}(\partial S/\partial \mathrm{N}_{\mathrm{mod}}) \right\rangle$ respectively. MC2P's k sensitivity, POE, PSE, and their relative standard deviations (SD) are in the third column. MC2P's relative errors to the analytic solutions are in the fourth columns in the table. The results agree well with the reference solutions within 95% confidence intervals.

Table 3.3 Comparisons of k sensitivities to the moderator density

Term	$\left(\partial k/\partial \mathrm{N}^{\mathrm{mod}}\right)_{\mathrm{REF}}$ a)	$\left(\partial k/\partial \mathrm{N}^{\mathrm{mod}}\right)_{\mathrm{MC2P}}$ (SD [%])	Relative Error [%]
Total	3.574×10^{-1}	3.597×10^{-1} (0.56)	0.64
1st-order POE	3.377×10^{-1}	3.384×10^{-1} (0.43)	0.21
1st-order PSE	1.969×10^{-2}	2.128×10^{-2} (6.64)	8.08

a) $\left(\partial k/\partial \mathrm{N}^{\mathrm{mod}}\right)_{\mathrm{REF}}$ is the analytic solution for $\partial k/\partial \mathrm{N}^{\mathrm{mod}}$

Table 3.4 shows the comparisons of k sensitivities to the macroscopic cross sections Σ of the fuel-coolant mixture and their POE and PSE. The first-order POE and PSE indicate $\left\langle (\partial \mathbf{H}/\partial \Sigma) S \right\rangle$ and $\left\langle \mathbf{H}(\partial S/\partial \Sigma) \right\rangle$ respectively. The first column shows the macroscopic cross sections of fuel-coolant mixture. Third and fourth columns show analytic solutions and MC2P calculation results. The fifth columns is for the relative errors of MC2P results to the reference solutions. From the table, one can see the MC2P's estimate shows good agreements with the analytic solutions within 95% confidence interval.

Table 3.4 Comparisons of k sensitivities to the macroscopic cross sections of fuel-coolant mixture, $\partial k/\partial\Sigma$, for the infinite homogeneous problem

Parameter x	Term	$(\partial k/\partial\Sigma)_{\mathrm{REF}}$ a)	$(\partial k/\partial\Sigma)_{\mathrm{MC2P}}$ (SD [%])	Relative Error[%]
Σ_{f1}	Total	7.240×10^{1}	7.241×10^{1} (0.01)	0.01
	1st-order POE	7.890×10^{1}	7.890×10^{1} (0.00)	0.00
	1st-order PSE	-6.494×10^{0}	-6.482×10^{0} (0.10)	0.18
Σ_{f2}	Total	3.164×10^{2}	3.164×10^{2} (0.00)	0.00
	1st-order POE	3.158×10^{2}	3.158×10^{2} (0.00)	0.00
	1st-order PSE	6.289×10^{-1}	6.309×10^{-1} (0.52)	0.32
$\Sigma_{\gamma1}$ b)	Total	-5.697×10^{1}	-5.697×10^{1} (0.00)	0.00
	1st-order POE	-5.708×10^{1}	-5.708×10^{1} (0.00)	0.00
	1st-order PSE	1.094×10^{-1}	1.084×10^{-1} (0.89)	0.91
$\Sigma_{\gamma2}$	Total	-3.235×10^{2}	-3.235×10^{2} (0.00)	0.00
	1st-order POE	-3.229×10^{2}	-3.229×10^{2} (0.00)	0.00
	1st-order PSE	-6.063×10^{-1}	6.046×10^{-1} (0.54)	0.28

a) $(\partial k/\partial\Sigma)_{\mathrm{REF}}$ is the analytic solution for $\partial k/\partial\Sigma$

b) $\Sigma_{\gamma g}=\Sigma_{tg}-\Sigma_{fg}-\sum_{g'}\Sigma_{sgg'}$

Table 3.5 and 3.6 show the comparisons of MC2P results of four terms in the right side of Eq. (14) for the second-order derivatives of k with respect to N^{mod} and Σ, denoted by $\partial^2 k/\partial N_{\mathrm{mod}}\partial\Sigma$, with analytic solutions. The terms of 2nd-order POE, 1st-order cross A, 1st-order cross B, and 2nd-order PSE in the table indicate $\left\langle\left(\partial^2\mathbf{H}/\partial\mathrm{N}_{\mathrm{mod}}\,\partial\Sigma\right)S\right\rangle$, $\left\langle\left(\partial\mathbf{H}/\partial\mathrm{N}_{\mathrm{mod}}\right)\cdot\left(\partial S/\partial\Sigma\right)\right\rangle$, $\left\langle\left(\partial\mathbf{H}/\partial\Sigma\right)\cdot\left(\partial S/\partial\mathrm{N}_{\mathrm{mod}}\right)\right\rangle$ and $\left\langle\mathbf{H}\left(\partial^2 S/\partial\mathrm{N}_{\mathrm{mod}}\partial\Sigma\right)\right\rangle$. From the table, one can see that the MC estimates of $\partial^2 k/\partial\mathrm{N}_{\mathrm{mod}}\partial\Sigma$ summing the four terms coincide with analytic solutions within 95% confidence intervals.

Table 3.5 Comparisons of the second-order k derivatives, $\partial^2 k/\partial \mathrm{N}_{\mathrm{mod}}\partial\Sigma$, for the infinite homogeneous problem

Parameter Σ	Term	$\left(\partial^2 k/\partial\Sigma\partial \mathrm{N}_{\mathrm{mod}}\right)_{\mathrm{REF}}$ a)	$\left(\partial^2 k/\partial\Sigma\partial \mathrm{N}_{\mathrm{mod}}\right)_{\mathrm{MC2P}}$ (SD [%])	Relative Error [%]
Σ_{f1}	Total	-6.140×10^{2}	-6.156×10^{2} (0.38)	0.26
	2nd-order POE	-7.019×10^{2}	-7.019×10^{2} (0.02)	0.00
	1st-order cross A	5.580×10^{1}	5.132×10^{1} (3.29)	8.03
	1st-order cross B	-2.539×10^{1}	-2.546×10^{1} (1.38)	0.28
	2nd-order PSE	5.749×10^{1}	6.041×10^{1} (2.52)	5.08
Σ_{f2}	Total	2.436×10^{2}	2.431×10^{2} (0.61)	0.21
	2nd-order POE	2.449×10^{2}	2.441×10^{2} (0.20)	0.33
	1st-order cross A	-5.428×10^{0}	-4.151×10^{0} (20.03)	23.53
	1st-order cross B	9.570×10^{0}	1.011×10^{1} (4.89)	5.64
	2nd-order PSE	-5.466×10^{0}	-6.931×10^{0} (13.68)	26.80

a) $\left(\partial^2 k/\partial \mathrm{N}_{\mathrm{mod}}\partial\Sigma\right)_{\mathrm{REF}}$ is the analytic solution for $\partial^2 k/\partial \mathrm{N}_{\mathrm{mod}}\partial\Sigma$

Table 3.6 Comparisons of the second-order k derivatives, $\partial^2 k/\partial \mathrm{N}_{\mathrm{mod}}\partial\Sigma$, for the infinite homogeneous problem

Parameter Σ	Term	$\left(\partial^2 k/\partial\Sigma\partial \mathrm{N}^{\mathrm{mod}}\right)_{\mathrm{REF}}$	$\left(\partial^2 k/\partial\Sigma\partial \mathrm{N}^{\mathrm{mod}}\right)_{\mathrm{MC2P}}$ (SD [%])	Relative Error [%]
$\Sigma_{\gamma 1}$ b)	Total	4.521×10^{2}	4.524×10^{2} (0.10)	0.07
	2nd-order POE	4.366×10^{2}	4.368×10^{2} (0.04)	0.05
	1st-order cross A	-9.399×10^{-1}	-5.537×10^{-1} (44.72)	41.09
	1st-order cross B	1.837×10^{1}	1.834×10^{1} (1.42)	0.16
	2nd-order PSE	-1.973×10^{0}	-2.140×10^{0} (11.89)	8.46
$\Sigma_{\gamma 2}$	Total	-1.588×10^{2}	-1.603×10^{2} (1.29)	0.94
	2nd-order POE	-1.599×10^{2}	-1.609×10^{2} (0.59)	0.63
	1st-order cross A	5.210×10^{0}	5.575×10^{0} (14.93)	7.01
	1st-order cross B	-9.783×10^{0}	-9.716×10^{0} (10.90)	0.68
	2nd-order PSE	5.682×10^{0}	4.797×10^{0} (19.97)	15.58

a) $\left(\partial^2 k/\partial \mathrm{N}_{\mathrm{mod}}\partial\Sigma\right)_{\mathrm{REF}}$ is the analytic solution for $\partial^2 k/\partial \mathrm{N}_{\mathrm{mod}}\partial\Sigma$

b) $\Sigma_{\gamma g}=\Sigma_{tg}-\Sigma_{fg}-\sum_{g'}\Sigma_{sgg'}$

Table 3.7 shows the comparisons for the sensitivities of the reactivity coefficient of the moderator number density to the fuel-coolant mixture cross sections, $\partial^2\rho/\partial \mathrm{N}_{\mathrm{mod}}\partial\Sigma$, calculated by Eqs. (2.12), (2.13) and (2.14) using the results of Tables 3.3, 3.4, 3.5 and 3.6 with analytic solutions. From the table, one can repeatedly see the MC2P method predicts the sensitivities

of the density coefficient with good agreements comparing with the analytic solutions.

Table 3.7 Comparisons of the sensitivities of the reactivity coefficient of the coolant number density to the macroscopic cross sections of fuel-coolant mixture for the infinite homogeneous problem

Parameter Σ	$\left(\partial^2\rho/\partial\Sigma\partial\mathrm{N}^{\mathrm{mod}}\right)_{\mathrm{REF}}$ a)	$\left(\partial^2\rho/\partial\Sigma\partial\mathrm{N}^{\mathrm{mod}}\right)_{\mathrm{MC2P}}$	Relative Error [%]
Σ_{f1}	-4.786×10^{2}	-4.799×10^{2} (0.35)	0.27
Σ_{f2}	3.684×10^{1}	3.605×10^{1} (4.06)	2.14
$\Sigma_{\gamma1}$ b)	3.540×10^{2}	3.543×10^{2} (0.10)	0.08
$\Sigma_{\gamma1}$	2.796×10^{1}	2.732×10^{1} (4.02)	2.29

a) $\left(\partial^2\rho/\partial\mathrm{N}_{\mathrm{mod}}\partial\Sigma\right)_{\mathrm{REF}}$ is the analytic solution for $\partial^2\rho/\partial\mathrm{N}_{\mathrm{mod}}\partial\Sigma$

b) $\Sigma_{\gamma g}=\Sigma_{tg}-\Sigma_{fg}-\sum_{g'}\Sigma_{sgg'}$

3.1.4. Sensitivity for reactivity coefficient of fuel temperature

The macroscopic cross sections are generated for the standard CANDU 6 lattice model at two different fuel temperatures which are 960.2K and 965.2K and given in Table 3.8. The ν_1, ν_2 values are set to 2.6649 and 2.4367 respectively. McCARD calculations are performed for 2,000 active cycles on 250,000 number of histories per cycle. The propagation batch size is set to 5.

Table 3.8 Two-group cross sections for the infinite homogeneous problem

Cross section	960.2K		XSs variation at 965.2K comparing with XSs at 960.2K[%]	
	Fast Gr.	Thermal Gr.	Fast Gr.	Thermal Gr.
Σ_{tg}	3.192×10^{-1}	4.379×10^{-1}	0.00058	-0.00040
$\Sigma_{\gamma g}$	1.383×10^{-3}	1.712×10^{-3}	-0.03640	-0.01898
Σ_{fg}	3.337×10^{-4}	1.765×10^{-3}	-0.00105	-0.02125
Σ_{s1g}	3.089×10^{-1}	6.600×10^{-5}	0.00043	-0.00024
Σ_{s2g}	8.627×10^{-3}	4.344×10^{-1}	0.00043	-0.00024
χ_{1g}	1.000	0.800	-	-
χ_{2g}	0.000	0.200	-	-

The MC2P calculation are performed varying the cross section, Σ. Table (3.9) shows the first-order *k* sensitivities and their relative errors to analytic solution. MC calculation results come with the relative SD in table. From the table, one can see that proposed method estimates the first-order *k* sensitivity with good agreements with analytic solutions within 95% confidence interval.

Table 3.9 Comparisons of k sensitivities to the macroscopic cross sections, $\partial k/\partial\Sigma$, for the infinite homogeneous problem

Parameter Σ	Term	$(\partial k/\partial\Sigma)_{\mathrm{REF}}$ a)	$(\partial k/\partial\Sigma)_{\mathrm{MC2P}}$ (SD [%])	Relative Error[%]
Σ_{f1}	Total	1.199×10^{2}	1.199×10^{2} (0.03)	0.00
	1st-order POE	1.242×10^{2}	1.242×10^{2} (0.01)	0.00
	1st-order PSE	-4.226×10^{0}	-4.247×10^{0} (0.77)	0.50
Σ_{f2}	Total	2.986×10^{2}	2.986×10^{2} (0.01)	0.00
	1st-order POE	2.982×10^{2}	2.982×10^{2} (0.00)	0.00
	1st-order PSE	4.055×10^{-1}	4.093×10^{-1} (3.08)	0.94
$\Sigma_{\gamma1}$ b)	Total	-8.936×10^{1}	-8.936×10^{1} (0.01)	0.00
	1st-order POE	-8.939×10^{1}	-8.939×10^{1} (0.01)	0.00
	1st-order PSE	2.974×10^{-2}	3.109×10^{-2} (14.28)	4.54
$\Sigma_{\gamma2}$	Total	-3.066×10^{2}	-3.066×10^{2} (0.00)	0.00
	1st-order POE	-3.062×10^{2}	-3.062×10^{2} (0.00)	0.00
	1st-order PSE	-3.990×10^{-1}	-3.995×10^{-1} (3.21)	0.13

a) $(\partial k/\partial\Sigma)_{\mathrm{REF}}$ is the analytic solution for $\partial k/\partial\Sigma$

b) $\Sigma_{\gamma g}=\Sigma_{tg}-\Sigma_{fg}-\sum_{g'}\Sigma_{sgg'}$

Table 3.10 shows the first-order k sensitivities to fuel temperature, T_f, calculated by MC2P and direct subtraction method with analytic solution. The McCARD calculation for the direct subtraction method is performed for 2,000 active cycles on 10,000,000 number of histories per cycle in two different temperature condition (955.2K and 965.2K). MC2P's k-sensitivity agrees very well with the reference solution while one estimated by the direct subtraction method show large discrepancy to the analytic solution with a large SD. It is note that four times more histories for the direct subtraction method compared to the MC2P are not enough to estimate the first-order k sensitivity to fuel temperature.

Table 3.10 Comparisons of k sensitivities to the fuel temperature

$\left(\partial k/\partial T_f\right)_{REF}$ a)	$\left(\partial k/\partial T_f\right)_{MC2P}$ (SD [%])	$\left(\partial k/\partial T_f\right)_{DIR}$ b) (SD [%])
-1.148×10^{-5}	-1.148×10^{-5} (0.56)	-2.785×10^{-6} (259)

a) $\left(\partial k/\partial T_f\right)_{REF}$ is the analytic solution for $\partial k/\partial T_f$

b) $\left(\partial k/\partial T_f\right)_{DIR}$ is the calculated by subtraction of k's from two different temperatures

The second-order derivatives of k with respect to Σ and T_f are calculated by MC2P. The MC2P results and their relative errors to analytic solutions are shown in Table 3.11 and 3.12. Further, Tables show the comparisons of four terms in the right side of Eq. (14) for the second-order derivatives of k with

respect to Σ and T_f, denoted by $\partial^2 k / \partial T_f \partial \Sigma$, with analytic solutions. The terms of 2nd-order POE, 1st-order cross A, 1st-order cross B, and 2nd-order PSE in the table indicate $\left\langle \left(\partial^2 \mathbf{H} / \partial T_f \partial \Sigma \right) S \right\rangle$, $\left\langle \left(\partial \mathbf{H} / \partial T_f \right) \cdot \left(\partial S / \partial \Sigma \right) \right\rangle$, $\left\langle \left(\partial \mathbf{H} / \partial \Sigma \right) \cdot \left(\partial S / \partial T_f \right) \right\rangle$ and $\left\langle \mathbf{H} \left(\partial^2 S / \partial T_f \partial \Sigma \right) \right\rangle$. From the table, one can see that the MC estimates of $\partial^2 k / \partial T_f \partial \Sigma$ summing the four terms coincide with analytic solutions within 95% confidence intervals.

Table 3.11 Comparisons of the second-order derivatives of k with respect to the fuel temperature and cross sections

Parameter Σ	Term	$\left(\partial^2 k/\partial\Sigma\partial \mathrm{T}_f\right)_{\mathrm{REF}}$ a)	$\left(\partial^2 k/\partial\Sigma\partial \mathrm{T}_f\right)_{\mathrm{MC2P}}$ (SD [%])	Relative Error [%]
Σ_{f1}	Total	-5.083×10^{-4}	-5.138×10^{-4} (0.72)	1.08
	2nd-order POE	-1.341×10^{-4}	-1.343×10^{-4} (0.14)	0.15
	1st-order cross A	-3.336×10^{-6}	-3.734×10^{-4} (0.69)	1.33
	1st-order cross B	-3.685×10^{-4}	-3.305×10^{-6} (17.43)	0.93
	2nd-order PSE	-2.341×10^{-6}	-2.841×10^{-6} (94.13)	21.36
Σ_{f2}	Total	1.051×10^{-2}	1.051×10^{-2} (0.03)	0.00
	2nd-order POE	1.045×10^{-2}	1.045×10^{-2} (0.01)	0.00
	1st-order cross A	1.278×10^{-6}	1.429×10^{-6} (51.11)	11.82
	1st-order cross B	3.536×10^{-5}	3.563×10^{-5} (2.91)	0.76
	2nd-order PSE	1.784×10^{-5}	1.874×10^{-5} (10.83)	5.04

a) $\left(\partial^2 k/\partial \mathrm{T}_f\partial\Sigma\right)_{\mathrm{REF}}$ is the analytic solution for $\partial^2 k/\partial \mathrm{T}_f\partial\Sigma$

Table 3.12 Comparisons of the second-order derivatives of k with respect to the fuel temperature and cross sections

Parameter Σ	Term	$\left(\partial^2 k/\partial\Sigma\partial \mathrm{T}_f\right)_{\mathrm{REF}}$ a)	$\left(\partial^2 k/\partial\Sigma\partial \mathrm{T}_f\right)_{\mathrm{MC2P}}$ (SD [%])	Relative Error [%]
$\Sigma_{\gamma 1}$	Total	1.952×10^{-3}	1.952×10^{-3} (0.04)	0.00
	2nd-order POE	1.947×10^{-3}	1.947×10^{-3} (0.01)	0.00
	1st-order cross A	2.402×10^{-6}	2.615×10^{-6} (16.86)	8.87
	1st-order cross B	2.594×10^{-6}	2.700×10^{-6} (13.23)	4.09
	2nd-order PSE	-1.302×10^{-7}	-3.545×10^{-7} (117.61)	172.27
$\Sigma_{\gamma 2}$	Total	-9.260×10^{-3}	-9.257×10^{-3} (0.05)	0.03
	2nd-order POE	-9.204×10^{-3}	-9.206×10^{-3} (0.03)	0.02
	1st-order cross A	-1.313×10^{-6}	-8.574×10^{-6} (184.54)	553.01
	1st-order cross B	-3.408×10^{-5}	-3.548×10^{-5} (2.98)	4.11
	2nd-order PSE	-1.507×10^{-5}	-1.440×10^{-5} (14.30)	4.45

a) $\left(\partial^2 k/\partial \mathrm{T}_f\partial\Sigma\right)_{\mathrm{REF}}$ is the analytic solution for $\partial^2 k/\partial \mathrm{T}_f\partial\Sigma$

b) $\Sigma_{\gamma g}=\Sigma_{tg}-\Sigma_{fg}-\sum_{g'}\Sigma_{sgg'}$

Table 3.13 shows the comparisons for the sensitivities of the reactivity coefficient of fuel temperature to the cross sections, $\partial^2\rho/\partial T_f\partial\Sigma$, calculated by Eqs. (2.12), (2.13) and (2.14) using the results of Tables 3.9, 3.10, 3.11 and 3.12 with analytic solutions. From the table, one can repeatedly see the MC2P method predicts the sensitivities of the fuel temperature coefficient with good agreements comparing with the analytic solutions.

Table 3.13. Comparisons of the sensitivities of the reactivity coefficient of fuel temperature to the macroscopic cross sections

Parameter Σ	$\left(\partial^2\rho/\partial T_f\partial\Sigma\right)_{REF}$	$\left(\partial^2\rho/\partial T_f\partial\Sigma\right)_{MC2P}$ (SD[%])	Relative Error [%]
Σ_{f1}	1.476×10^{-3}	1.471×10^{-3} (0.07)	0.34
Σ_{f2}	1.277×10^{-2}	1.277×10^{-2} (0.04)	0.00
$\Sigma_{\gamma1}$	1.147×10^{-4}	1.150×10^{-4} (0.41)	0.26
$\Sigma_{\gamma1}$	-1.193×10^{-2}	-1.192×10^{-2} (0.45)	0.08

a) $\left(\partial^2\rho/\partial T_f\partial\Sigma\right)_{REF}$ is the analytic solution for $\partial^2\rho/\partial T_f\partial\Sigma$

b) $\Sigma_{\gamma g}=\Sigma_{tg}-\Sigma_{fg}-\sum_{g'}\Sigma_{sgg'}$

3.2. ^{235}U−Density Coefficient in Godiva

The calculation efficiency of the MC2P method for the sensitivity estimate of the reactivity coefficient is examined for the reactivity coefficient of the ^{235}U number density in Godiva [16] by comparing with the Williams' method [13]. Godiva is a bare uranium sphere of a radius of 8.741 cm, consisting of 94.73 wt% ^{235}U and 5.27 wt% ^{238}U. The MC eigenvalue calculation adopting the MC2P method are performed on 2,000 active cycles with 10,000 histories per cycle using continuous-energy cross section libraries produced from ENDF/B-VII.1 [19]. The propagation batch size of 5 is used for the PSE calculations in the MC2P method. For the Williams' method calculations, the first-order k sensitivities to the ^{235}U and ^{238}U microscopic cross sections are calculated from the MC eigenvalue calculations for perturbed and unperturbed systems by the first-order DOS and FSP method. The MC k sensitivity calculations for the Williams' method are performed on 40,000 active cycles with 1,000,000 histories per cycle with varying the ^{235}U number density by 0.5%, 1% and 10%.

Tables 3.14 and 3.15 shows the comparisons of sensitivities of the ^{235}U-number-density coefficient to microscopic cross sections of ^{235}U and ^{238}U, respectively, between the MC2P method and the Williams' method. From the table, one can clearly see that the statistical uncertainty of the Williams method's results becomes larger as the ^{235}U number-density perturbation is

smaller and that, more importantly, the SDs of MC2P results are smaller than the Williams method's using 2,000 times bigger MC history simulations when the density perturbations are less than or equal to 1%. In addition to these, it is observed that the MC2P estimates agree well with the Williams method's using the ^{235}U number density perturbation of 1%.

Table 3.14. Comparisons of sensitivities of the ^{235}U-number-density coefficient to ^{235}U nuclear data for Godiva

^{235}U xs type, x	$(\partial^2\rho/\partial N^{235}\partial x)_{MC2P}$ (SD [%])	Williams' method		Rel. Diff. [%]
		ΔN^{235} [%]	$(\partial^2\rho/\partial N^{235}\partial x)_{Williams}$ (SD [%])	
ν	-6.25×10^{0} (0.04)	0.5	-6.44×10^{0} (0.37)	2.94
		1.0	-6.41×10^{0} (0.19)	2.90
		10.0	-5.85×10^{0} (0.02)	6.54
(n,γ)	-9.43×10^{-1} (0.27)	0.5	-8.14×10^{-1} (2.40)	13.69
		1.0	-8.12×10^{-1} (1.20)	13.93
		10.0	-7.58×10^{-1} (0.12)	19.64
(n,fis)	-1.44×10^{1} (0.05)	0.5	-1.46×10^{1} (0.23)	1.76
		1.0	-1.46×10^{1} (0.11)	1.40
		10.0	-1.33×10^{1} (0.01)	7.45
(n,n)	-3.05×10^{-1} (0.90)	0.5	-2.95×10^{-1} (2.70)	3.09
		1.0	-2.98×10^{-1} (1.34)	2.38
		10.0	-2.91×10^{-1} (0.13)	4.41
(n,n')	-8.67×10^{-1} (1.25)	0.5	-8.95×10^{-1} (2.92)	3.22
		1.0	-8.83×10^{-1} (1.48)	1.83
		10.0	-8.49×10^{-1} (0.15)	2.16

Table 3.15. Comparisons of sensitivities of the ^{235}U-number-density coefficient to ^{238}U nuclear data for Godiva

^{238}U xs type, x	$(\partial^2\rho/\partial N^{235}\partial x)_{MC2P}$ (SD [%])	Williams' method		Rel. Diff. [%]
		ΔN^{235} [%]	$(\partial^2\rho/\partial N^{235}\partial x)_{Williams}$ (SD [%])	
ν	-1.50×10^{-1} (0.04)	0.5	-1.50×10^{-1} (0.16)	0.57
		1.0	-1.50×10^{-1} (0.08)	0.01
		10.0	-1.31×10^{-1} (0.01)	12.47
(n,γ)	2.76×10^{-1} (0.05)	0.5	2.82×10^{-1} (0.38)	2.11
		1.0	2.80×10^{-1} (0.19)	1.64
		10.0	2.60×10^{-1} (0.02)	5.70
(n,fis)	-1.46×10^{0} (0.03)	0.5	-1.47×10^{0} (0.13)	0.50
		1.0	-1.46×10^{0} (0.06)	0.20
		10.0	-1.27×10^{0} (0.01)	12.79
(n,n)	-4.09×10^{-2} (1.33)	0.5	-4.37×10^{-2} (4.34)	6.84
		1.0	-4.16×10^{-2} (2.27)	1.69
		10.0	-3.69×10^{-2} (0.25)	9.79
(n,n')	-8.98×10^{-2} (1.54)	0.5	-8.32×10^{-2} (4.57)	7.41
		1.0	-8.73×10^{-2} (2.18)	2.78
		10.0	-7.90×10^{-2} (0.23)	12.13

Chapter 4. Applications for the Reactivity Coefficient S/U Analysis

4.1. Nuclear Data S/U Analysis

The uncertainty of the reactivity coefficient of parameter y due to multi-group covariance data can be calculated by the MC sandwich equation [20] using its sensitivities to cross sections as

$$\sigma^2\left[\partial\rho/\partial y\right]=\sum_{m,r}\sum_{m',r'}\sigma^2\left[\partial\rho/\partial y;x_r^m,x_{r'}^{m'}\right]; \tag{4.1}$$

$$\sigma^2\left[\frac{\partial\rho}{\partial y};x_r^m,x_{r'}^{m'}\right]=\sum_g\sum_{g'}\left(\mathrm{rcov}\left[x_r^m,x_{r'}^{m'}\right]\right)_{gg'}\cdot S_g\left[\frac{\partial\rho}{\partial y};x_r^m\right]\cdot S_{g'}\left[\frac{\partial\rho}{\partial y};x_{r'}^{m'}\right], \tag{4.2}$$

$$S_g\left[\frac{\partial\rho}{\partial y};x_r^m\right]=\int_{E_g}^{E_{g-1}}x_r^m(E)\frac{\partial^2\rho}{\partial x_r^m(E)\partial y}dE \quad , \tag{4.3}$$

where x_r^m denotes the continuous-energy cross section function, $x_r^m(E)$, of type r of nuclide m. $\mathrm{rcov}\left[X,Y\right]$ ($X=x_r^m(E)$, $Y=x_{r'}^{m'}(E')$) is the relative covariance between two uncertain cross sections X and Y and is defined as

$$\mathrm{rcov}\left[X,Y\right]=\frac{\mathrm{cov}\left[X,Y\right]}{E\left[X\right]\cdot E\left[Y\right]} \tag{4.4}$$

where $\mathrm{cov}\left[X,Y\right]$ is the covariance between X and Y and $E\left[\cdot\right]$ implies the expected value of a variable in the brackets. $\left(\mathrm{rcov}\left[x_r^m,x_{r'}^{m'}\right]\right)_{gg'}$ means the

relative covariance between the cross section x_r^i for a neutron with energy E in the g-th group $[E_g, E_{g-1})$ and the cross section $x_{r'}^{i'}$ for a g'-th group neutron in the energy interval of $[E_{g'}, E_{g'-1})$. In this study, the multi-group covariance data of $\left(\mathrm{rcov}\left[x_r^m, x_{r'}^{m'}\right]\right)_{gg'}$ are produced in the SCALE 44-group structure [21] from ENDF/B-VII.1 by NJOY99 [22]. Then the group-wise sensitivities of $\partial\rho/\partial y$ to cross section x_r^m, $S_g\left[\partial\rho/\partial y; x_r^m\right]$ defined by Eq. (4.3), are calculated by the proposed MC2P method.

4.2. MDC S/U Analysis for Continuous-Energy PWR Pin Problem

The MDC uncertainty due to the nuclear covariance data is estimated by Eqs. (4.1), (4.2), and (4.3) using the MC2P method for the TMI-1 pin cell problem which is one of the OECD benchmarks for uncertainty analysis modeling (UAM) for design, operation, and safety analysis LWRs [23]. The TMI-1 pin cell problem is composed of 4.85 w/o enriched UO_2 pellet inside the Zircaloy-4 cladding and the surrounding water moderator. The McCARD eigenvalue calculations are performed on 20,000 active cycles with 10,000 histories per cycle using the continuous-energy cross section libraries from ENDF/B-VII.1. In the MC2P perturbation calculations, the propagation batch size is set to 5. Table 4.1 shows the contributions of the cross section uncertainties of ^{235}U and ^{238}U to the MDC uncertainty. The

SDs of the covariance type-wise and the total uncertainties are calculated by the Gelbard and Prael's non-overlapping batch method [24] with the batch size of 200 active cycles. The MDC of the TMI-1 pin cell problem is estimated as 0.134 $(\Delta\rho)/(g/cm^3)$ with its SD of 0.42% by the first-order DOS and FSP methods. From the table, one can see that the uncertainty of the MDC in the TMI-1 pin cell problem is 0.44% due to the ^{235}U and ^{238}U covariance data and the covariances between the (n,n') and (n,n') cross sections of ^{238}U are dominating contributors to the MDC uncertainty.

Table 4.1 MDC uncertainties, $\sigma\left[\partial\rho/\partial D_M ; X, X'\right]$, due to the covariance in ^{235}U and ^{238}U ENDF/B-VII.1 for the TMI-1 pin cell problem

Nuclide	Covariance Type	$\sigma\left[\partial\rho/\partial T_f ; X, X'\right]$ [%] (SD) [%]
^{235}U	ν, ν	0.005 (0.30)
	(n,γ), (n,γ)	0.237 (0.16)
	(n,γ), (n,n)	0.020 (4.52)
	(n,fis), (n,fis)	0.007 (2.21)
	(n,n'), (n,n')	0.012 (4.62)
^{238}U	(n,γ), (n,γ)	0.037 (0.41)
	(n,fis), (n,fis)	0.008 (6.69)
	(n,n), (n,n)	0.136 (6.03)
	(n,n), (n,n')	0.170 (5.57)
	(n,n), $(n,2n)$	0.009 (6.20)
Total		0.44 (3.01)

4.3. FTC S/U Analysis for Continuous-Energy CANDU 6 Bundle Problem

The FTC uncertainty caused by the 44-group covariance data of ^{235}U and ^{238}U is estimated by Eqs. (4.1) and (4.2) for the CANDU 6 bundle model [16] described in Chapter 2. The sensitivity of the FTC to cross section, $\partial^2\rho/\partial x_r^m \partial \mathrm{T}_f$ is calculated by converting it to the corresponding derivatives of the microscopic cross sections of and the transfer probability functions of

neutrons undergoing scattering collisions by constituent isotopes of fuel regions [9] as it is described in sub-chapter 2.6. The MC eigenvalue calculation applying the MC2P method with the propagation batch size of 5 is performed on 20,000 active cycles with 10,000 histories per cycle using the continuous-energy cross section libraries from ENDF/B-VII.1. Table 4.2 shows the FTC uncertainties due to the cross section uncertainties of ^{235}U and ^{238}U. The FTC of the fresh-state CANDU 6 lattice problem is calculated as -1.101 pcm/K with its SD of 2.42%. From the table, one can see that the uncertainty of the FTC in the CANDU 6 lattice cell due to the ^{235}U and ^{238}U covariance data is 1.24% of which main contributors are the covariances of "(n,n'), (n,n')", "(n,n), (n,n')", and "(n,n), (n,n)" of ^{238}U.

Table 4.2 FTC uncertainties, $\sigma\left[\partial\rho/\partial T_f; X, X'\right]$, due to the covariance in ^{235}U and ^{238}U ENDF/B-VII.1 for the CANDU 6 lattice cell problem

Nuclide	Covariance Type	$\sigma\left[\partial\rho/\partial \mathrm{T}_f; X, X'\right]$ [%] (SD [%])
^{235}U	$\nu,\ \nu$	0.001 (9.04)
	$(n,\gamma),\ (n,\gamma)$	0.007 (3.77)
	$(n, fis),\ (n, fis)$	0.003 (5.14)
	$(n,n),\ (n,n)$	0.020 (5.46)
	$(n,n'),\ (n,n')$	0.021 (5.96)
^{238}U	$(n,\gamma),\ (n,\gamma)$	0.033 (2.51)
	$(n, fis),\ (n, fis)$	0.086 (7.47)
	$(n,n),\ (n,n)$	0.701 (5.42)
	$(n,n),\ (n,n')$	0.680 (5.69)
	$(n,n),\ (n,2n)$	0.039 (6.51)
	$(n,2n),\ (n,2n)$	0.096 (7.31)
	$(n,n'),\ (n,n')$	1.041 (6.17)
total		1.24 (6.38)

Chapter 5. Conclusions

In this study, the second-order DOS/FSP formulation for two different variables adequate to estimate sensitivities of the reactivity coefficients is derived. The sensitivity of reactivity coefficient are composed of the first-order and second-order derivative of k terms. The first-order derivatives are expressed as the sum of the first-order POE and PSE. The second-order derivatives are expressed as the sum of the second-order POE, PSE, and two cross terms. The first-order or second-order POE can be estimated by using the DOS method [3, 14], while the first-order and second-order PSE terms can be obtained by the FSP method [13]. The cross terms can be obtained by the first-order DOS/FSP method. The proposed MC2P algorithm implemented in the multi-group and/or continuous-energy MC code, McCARD, and is tested for an analytic two-group infinite homogeneous problem. The cross section sensitivities of the moderator density coefficient and fuel temperature coefficient of the two-group homogeneous problem estimated by the MC2P method agree well with analytic solutions within their 95% confidence intervals.

The superiority of MC2P method to the existing direct subtraction approach is demonstrated from the cross section sensitivity calculations of the ^{235}U density coefficient in Godiva. From the comparison results, one can see that the new method can predict the cross section sensitivities of the reactivity

coefficient more accurately from much smaller number of MC history simulations. In addition, the proposed method is applied for the S/U analyses of the MDC in a TMI-1 pin cell problem and the FTC of a CANDU 6 lattice cell problem for the ^{235}U and ^{238}U covariance data. The uncertainty contribution of the covariance between inelastic reaction and inelastic reaction of ^{238}U is dominant. It contributes to the uncertainty as much as 0.34% of MDC. Total uncertainty of MDC due to ^{235}U and ^{238}U cross section uncertainties is 0.44%. Next, in the CANDU 6 bundle problem, the FTC uncertainty due to ^{235}U and ^{238}U nuclear covariance data are estimated. The uncertainty contribution of the covariance between inelastic reaction and inelastic reaction of ^{238}U is dominant. It contributes to the uncertainty as 1.04% of FTC. Total uncertainty of FTC is 1.24%. S/U analysis using MC2P is done for MDC and FTC successfully.

Reference

1. T. E. Schaubel, “CNSC Staff Review of Pickering NGS-B Integrated Safety Review –Safety Analysis Safety Factors Report,” Letter to D. P. McNeil, April 7, 2008, E-Docs #3232348 (2008).
2. Y. Kim, D. Hartanto, W. Kim, “A Lattice-Based Monte Carlo Evaluation of Canada Deuterium uranium-6 Safety parameters,” *Nucl. Eng. Technol*., 48, 642 (2016).
3. H. Rief, “Generalized Monte Carlo perturbation algorithms for correlated sampling and a second-order Taylor series approach.” *Ann. Nucl. Energy*, 11. 455 (1984).
4. Y. Nagaya, T. Mori. “Impact of perturbed fission source on the effective multiplication factor in Monte Carlo perturbation calculations.” *Journal of nuclear science and technology* 42.5 (2005): 428-441.
5. E. Greenspan, “Developments in Perturbation Theory” *Advances in Nuclear Science and Technology*, **9**, 181 (1976).
6. M. L. Williams, “Perturbation Theory for Nuclear Reactor Analysis,” *CRC Handbook of Nuclear Reactors Calculations*, Vol. III, CRC Press, Inc., Boca Raton, FL (1986).
7. H. J. Shim, C. H. Kim, “Adjoint Sensitivity and Uncertainty Analyses in Monte Carlo Forward Calculations.” *J. Nucl. Sci. Technol*., 48[12], 1453 (2011).

8. B. C. Kiedrowski and F. B. Brown, “Adjoint-Based *k*-Eigenvalue Sensitivity Coefficients to Nuclear Data Using Continuous-Energy Monte Carlo,” *Nucl. Sci. Eng.*, **174**, 227 (2013).

9. H. J. Shim, C. H. Kim, “Monte Carlo fuel temperature coefficient estimation by an adjoint-weighted correlated sampling method.” *Nuclear Science and Engineering* 177.2 (2014): 184-192.

10. D. G. Cacuci, *Sensitivity and Uncertainty Analysis, Volume I: Theory*, Chapman & Hall/CRC (2003).

11. D. Rochman, A. J. Koning, D. F. Da Cruz, “Uncertainties for the Kalimer Sodium Fast Reactor: Void Reactivity Coefficient, k_{eff}, β_{eff}, Depletion and Radiotoxicity,” *J. Nucl. Sci. Technol.*, **48**[8], 1193 (2011).

12. Williams, M. L. "Sensitivity and uncertainty analysis for eigenvalue-difference responses." *Nuclear science and engineering* 155.1 (2007): 18-36.

13. Y. Nagaya, T. Mori, “Estimation of Sample Reactivity Worth with Differential Operator Sampling Method,” *Prog. Nucl. Sci. Technol.*, **2**, 842 (2011).

14. B. Morillon, “On the use of Monte Carlo perturbation in neutron transport problems,” *Ann. Nucl. Energy*, **25**, 1095 (1998).

15. H. J. Shim, B. S. Han, J. S. Jung. H. J. Park, C. H. Kim, “McCARD: Monte Carlo Code for Advanced Reactor Design and Analysis,” *Nucl. Eng. Technol.*, **44**[2], 151 (2012).

16. *International Handbook of Evaluated Criticality Safety Benchmark Experiments*, NEA/NSC/DOC(95)03, OECD Nuclear Energy (2006).
17. Seung Yeol Yoo, Hyung Jin Shim, and Chang Hyo Kim, "Monte Carlo Few-Group Constant Generation for CANDU 6 Core Analysis," *Science and Technology of Nuclear Installations*, vol. 2015, Article ID 284642, 11 pages, 2015. doi:10.1155/2015/284642.
18. J. Lieberoth, "A Monte Carlo Technique to Solve the Static Eigenvalue Problem of the Boltzmann Transport Equation," *Nukleonik*, **11**, 213 (1968).
19. M. B. Chadwick et al., "ENDF/B-VII.1 Nuclear Data for Science and Technology: Cross Sections, Covariances, Fission Product Yields and Decay Data," Nuclear Data Sheets, 112 (12), 2887 (2011).
20. D. H. Lee, H. J. Shim, C. H. Kim, "Monte Carlo Sensitivity and Uncertainty Analysis with Continuous-Energy Covariance Data," *Nucl. Sci. Eng.*, **187** [2], 154-165 (2017).
21. ZZ SCALE6.0/COVA-44G, "44-group cross-section covariance matrix library extracted from SCALE6.0," NEA Data Bank, USCD-1236/02 (2009).
22. R. E. MacFarlane, D. W. Muir, "NJOY99.0 Code System for Producing Pointwise and Multigroup Neutron and Photon Cross Sections from ENDF/B Data," PSR-480/NJOY99.0, Los Alamos National Laboratory (2000).
23. K. Ivanov, M. Avramova, S. Kamerow, I. Kodeli, E. Sartori, E. Ivanov,

O. Cabellos, “Benchmark for Uncertainty Analysis in Modeling (UAM) for Design, Operation and Safety Analysis of LWRs, Volume I: Specification and Support Data for the Neutronics Cases (Phase I),” NEA/NSC/DOC(2012), OECD Nuclear Energy Agency (2012).

24. E. M. Gelbard and R. Prael, “Computation of Standard Deviations in Eigenvalue Calculations,” *Prog. Nucl. Energy*, **24**, 237 (1990).

25. J. F. Briesmeister, “MCNP-a general Monte Carlo N-particle transport code, version 4B,” LA-13181, *Los Alamos National Laboratory* (1997).